construction materials

MDPI

Article

Blistering of Reactive Resin Coatings on Concrete: New Insights

Franziska Vogt * and Andrea Osburg

F. A. Finger-Institute for Building Materials Science, Bauhaus-Universität Weimar, 99423 Weimar, Germany; andrea.osburg@uni-weimar.de

* Correspondence: franziska.vogt@uni-weimar.de; Tel.: +49-3643-584932

Abstract

The formation of blisters in reactive resin coatings on concrete is a widely known phenomenon that is also a subject of debate in the literature. In particular, blisters forming after curing of the coating can lead to extensive damage. This study was focused on the investigation of blistering between the concrete substrate and the resin coating. The hypothesis is that the cementitious material and the overlying reactive resin coating form a system that leads to damage under certain boundary conditions regarding material composition, as well as moisture and mass transport. Systematic investigations were carried out in an extensive testing program with various substrate mortars that differ in cement type, water–cement ratio, and aggregate. As coating systems, two different EP primers were used with a transparent EP topcoat. The long-term testing was conducted on potential blistering of composite test specimens stored under various (practically relevant) conditions prior and after the coating. It was found that a higher moisture content of the substrate reduces blistering of the EP coating system. EP systems containing benzyl alcohol do not automatically tend to blister. Furthermore, condensation in the substrate provides sufficient amounts of water to cause blistering and ASR can contribute to blister formation.

Keywords: resin coating; epoxy; concrete; transparent coating; blistering; blister area ratio; leaching tests; osmotic processes; ASR

1. Introduction

Reactive resin coatings have been used for many decades to protect concrete components from damage caused by mechanical influences and/or corrosive media. Since the 1970s, the occurrence of blistering of resin coatings on concrete is known (e.g., [1,2]), and numerous studies have been carried out to clarify the causes. The problem is highly significant as in these cases the entire coating system must be replaced, resulting in considerable economic losses. A distinction is made between blisters that form in the fresh, uncured coating system and those that appear when the coating has cured. The period for the formation of such subsequent blisters extends from a few days to possibly years after application or curing. In the following, only subsequently formed blisters that result from moisture in the substrate are discussed.

In the literature, there is a disagreement about the causes of blister formation. Generally, the origin of the damaging causes has been looked for in the coating systems, the concrete substrate, as well as in external influencing factors and transport processes. Examples include high solvent content in the coating systems, hydrostatic pressure, excess pressure due to capillary action, corrosion phenomena or osmotic processes. However, osmotic blister formation in particular is highly controversial because it has not yet been

Received: 3 March 2026
Revised: 23 April 2026
Accepted: 12 May 2026
Published: 19 May 2026

proven or disproven beyond doubt [3], although Schulenberg [4] was able to demonstrate that cement mortars can act as semipermeable membranes.

The following paragraphs examine influencing factors and observations in connection with blister formation.

According to Wolff [5], possible causes for blistering from primers and epoxy resin coatings are cross-linking defects or perforations in the primer. Specifically, he refers to segregation phenomena (e.g., due to chromatographic effects), the use of non-reactive solvents, and incorrect mixing ratios. The latter was not considered by Schäper and Wächter [6] to significantly increase damage. However, they found that a high degree of cross-linking before the onset of moisture penetration contributes significantly to the prevention of blistering. Experiments conducted by Schäper et al. [7] showed that blistering did not occur in sanded primers despite particularly unfavorable conditions. Wolff [5], on the other hand, saw perforation of the primer as a possible cause of damage due to the use of excessively coarse sanding. However, Schäper and Wächter [6] were able to show, through comparative tests with glass beads, that at least the grain shape and thus possible perforations of the primer have no significant influence on blistering. Another influence on the appearance of delamination of epoxy coatings is their tendency to swell when they come into contact with water, thereby changing their properties (e.g., adhesion, elasticity, and glass transition temperature), which can promote local delamination and subsequent bulging [6,8]. Organic solvents can cause damage to coatings even in low concentrations [9]. Gaiser [10] already considered this to be state of the art in 1991. Even though solvents are no longer frequently used [11], solvent-based epoxy resin systems are still available on the market due to their better workability and lower costs. It is also common practice to add solvents during the application of a coating system to improve workability or to increase the penetration depth of the primer into the concrete. According to Wolff and Raupach [12], benzyl alcohol has a particularly negative effect in this regard. Reactive diluents are considered relatively unproblematic, as they only insignificantly alter the properties of the cross-linked end product [13]. Nevertheless, unreacted reactive diluents have been found in blister fluids [14,15] and are suspected to act as blister nuclei [16,17].

The findings on the influence of concrete compressive strength on blister formation in reactive resin coatings differ greatly. Particularly in older publications, increased blistering is observed with increasing concrete strength class (above C35/45). Stenner and Machill [18], on the other hand, identified concrete of lower strength classes (C30/35 and below) as particularly promoting blistering. In the numerous studies in laboratories and reports on blister formation in buildings, many cement-based substrate materials were considered that varied in composition and compressive strength. The following provides an overview of the influences of strength and w/c ratio on blister formation as reported in the literature. Rheinwald [19] found that blisters mainly occur on concretes of strength classes B35, B40, and B45 (corresponding to C30/37, C35/45, respectively); less frequently in concretes of lower strength (B25 (corresponding to C20/25)). In a later publication, Rheinwald [20] described an example of an affected underground car park with concrete of strength class B35 (corresponding to C30/37). According to Fiebrich [17], higher-strength concretes (B55 (corresponding to C45/55)) show more blistering with solvent-based epoxy (EP) systems. Hensel [21] found that fiber cement panels and B55 concrete were more susceptible than B15 (corresponding to C12/15). According to Raddatz and Stenner [14], pressure cannot build up in low-strength concrete because its porosity is relatively high and the pressure can be equalized in the pore system. Stenner and Machill [18] observed blistering only with B25 (corresponding to C20/25) and no blisters with B55 (corresponding to C 45/55), even after 28 months. Yuasa et al. [22,23] compared concretes with w/c ratios of 0.4 to 0.8 and found that low w/c ratios and thus higher strengths result in reduced

blistering. Wolff [24] considered C50/60 less critical in terms of alkali diffusion toward the coating due to its lower capillary porosity than C20/25, which has a high capillary porosity. Bode et al. [3] observed blistering in C25/30 and determined alkali–silica reaction (ASR) as the cause. According to Schäper and Wächter [6], concrete with w/c ratios below 0.6 prevents blistering by reducing capillary suction.

Several studies have examined the influence of storage and pretreatment of concrete prior to coating. According to Yuasa et al. [22], concrete samples that are stored under water are less susceptible to blistering than samples that are initially stored dry and then wet. Schäper and Kreye [25] also saw an increased likelihood of blistering in heavily dried-out concrete (moisture content < 4%) that is suddenly exposed to moisture. This is explained by increasing capillary pressure due to rising water. However, this pressure cannot develop to the same extent in capillary pores that are already filled with water. In other cases, a too-high moisture content of the concrete prior to coating was identified as a cause for blistering, e.g., [26]. It has long been known that coatings on shot-blasted concrete surfaces show less blistering than on untreated surfaces. The weaker cement-rich surface is removed, which significantly improves the adhesive bond between the concrete and the coating [17,26]. It can also be assumed that accumulations such as carbonates, sulfates, or components of concrete admixtures are removed from the surface, which can significantly reduce possible interactions with the coating.

The concept of osmotic blistering with water supplied from the substrate has long been discussed in the literature, e.g., [3,4,9,22,27–39]. In general, the following four factors are described as prerequisites for this: (1) the presence of liquid water, (2) formation of a semipermeable membrane, (3) presence of water-soluble substances as the cause of the concentration difference, and (4) formation of a pressure-tight cell. Wolff et al., who published various papers on blistering, ruled out osmosis as the cause for blistering [5,12,40]. However, their underlying argument is flawed, as it assumes that the necessary semipermeable membrane is only permeable to the solvent, which is incorrect. Schulenberg [4] conducted experiments in which the measured concentrations of dissolved salts in the concentrated solution were lower at the end of the experiment than at the beginning (Figure 1), which can be explained by the transport of ions toward the deionized water and by interactions of the dissolved ions with the sample. At the same time, water molecules migrate from the half-cell of the pure solvent toward the concentrated solution and dilute it. Schulenberg [4] has shown that cement mortar with a water-to-cement ratio of between 0.45 and 0.60 acts as a semipermeable membrane and can cause osmotic pressures of up to 0.1 N/mm^2. Furthermore, it was found that the semipermeable membrane is not a distinct layer of the sample, but rather that the entire mortar body acts as such a membrane.

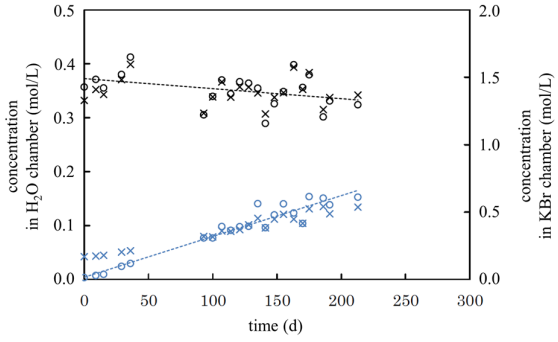

Figure 1. Diffusion experiment with w/c 0.6; concentration curve of bromine (circle) and potassium (cross) in the chamber of the pure solvent (blue) and the concentrated solution (black); based on Schulenberg [4].

Another type of osmotic blistering occurs when the moisture pressure acts from the coated side. In that case, the coating itself acts as a semipermeable membrane. Blisters can form between the topcoat and the primer, or between the coating system and the substrate. Causes of this include, among others, the selection of an unsuitable coating material, improper application, loss of elasticity, and deterioration of mechanical properties, as well as surface damage of the coating material during use, e.g., [41,42]. This is undoubtedly a major problem, particularly in tank construction, swimming pools, and water treatment plants. However, in this study, we examined cases in which moisture acts from the substrate side.

Wolff [5] did not see any significant influence of osmotic transport processes on the blistering of coating systems, but, like Günter [16], suspected excess pressure in the capillary structure, which is sufficient to cause local delamination if the bond between the concrete and the primer is weakened in certain areas. In tests with standing water, Günter [16] found overpressures of around 0.3 N/mm^2. Aher et al. [39] contradicted the above: in their study, no air overpressure in the concrete/coating interface due to capillary water absorption in the substrate could be detected. There is a consensus in the literature that most pressures that can arise under a coating (approximately 0.3 N/mm^2 for capillary pressures [16]) do not exceed the adhesive strength (at least 1.5 N/mm^2 [43]) of properly applied coatings [5,16]. However, local disturbances in the interface can cause stresses 10 times higher to develop in the area of this disturbance [44]. In order to determine the critical pressure as a function of the defect radius, Günter [44] applied the so-called blister test to coated mortar panels. The smaller the defect diameter, the greater the pressure below the coating had to be to form a blister. However, according to Günter's calculations, the capillary pressure is sufficient to achieve stresses of 3 N/mm^2 between the concrete and the coating in the case of a defect with a diameter of 1 cm, thus forcing blister formation and growth. The maximum stresses he specified were reached after a maximum of 2 months and then remained constant for several months.

Pfaff and Gelfant [32] examined coatings on concrete damaged by blistering for signs of damaging alkali–silica reaction (ASR). However, no evidence of this damage mechanism was found. Some authors cite the ASR as a rare but possible cause of blistering on coating systems [28,37,45,46]. However, some only see this in combination with osmotic processes [28]. Rheinwald [45], on the other hand, makes a strict distinction between the two phenomena, but admits that the distinction is sometimes very difficult to make. Molkenthin et al. [46] also point out that the significance of ASR in damage cases is often underestimated. They investigated whether interactions occur between the reaction products of ASR and solvent-based or aqueous primers, but were unable to establish any connection. They attributed this to the insufficient contact time between the solvents and the silicic acids. Wolff et al. [47] observed that a coating can bulge locally in the form of blisters due to near-surface ASR in concrete on an offshore structure where reactive aggregates were used. However, the literature dealing with blistering generally does not address the aggregate used in concrete and its alkali sensitivity. The silicates required for ASR do not necessarily have to come from reactive aggregates. Other possible sources of silicate are setting accelerators or surface hardeners based on water glass. There are studies that show that the use of reactive aggregates can trigger ASR under a coating, which subsequently induces bulging of the coating or blistering [3,34]. The use of water glass-based surface hardeners resulted in more extensive delamination without bulging [34]. In the case of ASR, increased reactivity of the ASR gel can be expected as temperatures rise [3,48,49]. With constant humidity and rising soil temperature, it can therefore be assumed that damage will occur more quickly and more severely [3]. Molkenthin et al. [46] used laser-induced breakdown spectroscopy (LIBS) in their investigations to obtain an elemental mapping of a sample cross-section. They found an accumulation of potassium ions beneath the coating.

Such alkali enrichment on the surface can trigger or promote ASR and may explain the damage to the concrete, which is often limited to the area close to the surface.

The carbonation of concrete begins upon contact with air. The hydroxide ions present in the cement stone react with the carbon dioxide in the air and form carbonate salts such as (Na,K)HCO_3 and $CaCO_3$, with an increase in volume and a decrease in pH value. Hensel [21] considers that carbonates are partly responsible for the osmotic pressures that develop under coating systems, as they can form a semipermeable layer for alkali hydroxides by narrowing the pores. Hofmann [50] used energy-dispersive X-ray spectroscopy (EDX) to detect calcium carbonate in samples damaged by blistering, particularly in the blister area, which suggests a connection with the cause of the damage. Schäper et al. [7], on the other hand, found no blistering whatsoever in carbonated concrete of strength class C50/60 with an average carbonation depth of 5 mm.

The key aspect of this study was systematic long-term testing on blistering of composite test specimens stored under different conditions prior to and after coating. The results of previous research into blistering in the composite system of cementitious material and reactive resin coating are, in some cases, highly contradictory. Analysis shows that either the boundary conditions of the experiments were very different or the experiments and their results and interpretation were not described in sufficient detail, meaning that the causes of the differing results cannot be identified. The aim of this study was to resolve the contradictions in the literature through systematic model experiments, thereby ruling out certain aspects or confirming others with greater certainty. Unlike many other studies, this research was focused exclusively on blisters forming between the substrate and the coating system when moisture is present from within the substrate or from beneath it. The study was based on osmotic processes, whereby, in the aforementioned case, it is not the coating system or the primer that acts as a semipermeable membrane, but rather the osmotic processes take place within the substrate itself [4]. The aim was to clarify how the environmental conditions influence blister formation in order to more reliably derive prevention strategies. To achieve this, four varying mortars were used to record the effects of different base materials. In addition, two different coating materials were used to identify their effects. The materials were extensively characterized and the manufacturing conditions were kept constant in order to record or to rule out any influences from these factors, respectively.

2. Materials and Methods

The experimental program involved initial investigations into the properties of the reactive resin systems and cementitious materials used as substrates for corresponding coatings. Subsequently, composite samples of coated substrate slabs were examined for blister formation under various boundary conditions that simulated practical environmental conditions. For this purpose, the samples were exposed to different storage conditions before and after the coating. Transparent coating systems enabled immediate visual detection of signs of delamination and provided insights into the location and timing of blister formation.

2.1. Materials

As substrate materials for the composite samples, different mortars were used as substitutes for the concretes typically used in practice, as they are more homogeneous. With the help of mortars of different properties, the main influencing factors from the cementitious material on blistering of the resin coating could be recorded.

Two types of Portland cement were used for the substrate mortars. One was an ordinary Portland cement (CEM I 42.5 R) with a high alkali content, and the other was

a Portland cement with a low effective alkali content (CEM I 42.5 R-SR 0). These two cement types were selected specifically to investigate the effects of ASR on blister formation. Table 1 shows the most important properties of the cements and Table 2 their chemical compositions, which were determined using inductively coupled plasma optical emission spectrometry (ICP-OES, see Section 2.2.1).

Table 1. Properties of cements.

	Density (kg/m^3)	Specific Surface (cm^2/g)	Sodium Equivalent (-)
CEM I 42.5 R	3100	4300	1.23
CEM I 42.5 R-SR 0	3200	4090	0.54

Table 2. Chemical composition of cements.

Chemical Component		CaO	SiO_2	Al_2O_3	Fe_2O_3	SO_3	MgO	K_2O	Na_2O	LOI *
CEM I 42.5 R	(wt.%)	63.3	20.2	4.8	2.6	3.0	1.5	1.31	0.37	2.7
CEM I 42.5 R-SR 0	(wt.%)	61.5	19.8	4.4	6.9	2.2	0.8	0.6	0.15	2.7

* LOI—Loss on Ignition.

The clinker phases, as shown in Table 3, can be calculated from the chemical composition using the Bogue equation [51]. The values shown are reference values; deviations from 100% occur because free lime, gypsum, and foreign oxides are not taken into account in the formulas.

Table 3. Clinker phases of cements.

		C_3S	C_2S	C_3A	C_4AF
CEM I 42.5 R	(%)	59.6	13.0	8.3	7.9
CEM I 42.5 R-SR 0	(%)	54.1	15.9	0.0	21.0

As coating systems, two commercially available epoxy (EP) resin primers with the same EP topcoat were used. The authors have found that most damage cases occurred with similar systems that were used in this study. EP1 is a solvent-free, colorless two-component (resin and hardener) epoxy resin containing benzyl alcohol as reactive thinner. It is a proven product and is used in practice for primers, scratch coats, mortar and leveling layers. EP2 is a colorless two-component epoxy resin containing no benzyl alcohol. As it has very low-emission properties, it is especially suitable for application in living quarters. The EP topcoat is also a solvent-free two-component epoxy resin with low-emission properties. It was applied without any filler in order to be able to visually assess any reactions taking place underneath the transparent coating system. The solid content and the density of the EP resins are presented in Table 4.

Table 4. Properties of the EP resins.

		EP1	EP2	EP Topcoat
Solid Content	(%)	99	99.8	100
Density	(kg/m^3)	1100	1100	1080

The resin and hardener of the primers, as well as of the topcoat, were mixed mechanically at approximately 400 rpm using a slow-running laboratory mixer. Mixing time was 2 to 3 min until a homogeneous, streak-free mass was formed. To avoid mixing errors, the

resin/hardener mixture was then transferred to a clean container and mixed again briefly. Mixing of the EP resins and sample preparation was always conducted at 20 °C.

The substrate mortars varied in terms of cement type, water-to-cement ratio (w/c), and aggregate. Table 5 summarizes the composition of the mortars and their designations.

Table 5. Mix designs of the substrate mortars.

Sample ID	CEM I 42.5 R (kg/m^3)	CEM I 42.5 R-SR 0 (kg/m^3)	w/c Ratio	Vol. Aggregate-to-Binder Ratio
M1	500	-	0.55	3.51
M2	-	500	0.55	3.51
M4	-	500	0.40	3.51
M7	500	-	0.55	3.51

Mortars M1 and M2 varied in cement type. Based on M2, another mortar was designed with a lower w/c ratio—M4. In all these mortars, CEN Standard Sand EN 196-1 (0.08/2.0 mm) [52] was used as aggregate. This is a standardized sand with a constant grain size distribution, produced from natural quartz sand with particles of a generally rounded shape. It is mainly used for standardized cement testing and was selected for this study to ensure homogeneous substrate mortars throughout the investigations and to rule out any unintended influences from aggregates on blister formation. Mortar M7 was designed specifically to investigate the influence of alkali–silica reaction on blister formation by substitution of the aggregate fraction 1.6/2.0 mm with soda-lime glass balls with a diameter of 2 mm and with a density of 2580 kg/m^3. In Table 6, the chemical components of the glass balls according to the data sheet are summarized. To ensure comparability, the mortars were designed with an identical volumetric aggregate-to-binder ratio of 3.51.

Table 6. Chemical components of the glass balls, %.

SiO_2	Na_2O	Al_2O_3	K_2O	B_2O_3	BaO	CaO	MgO
69	13	4	3	1	2	5	3

The substrate mortars were prepared using a Zyklos Rotating Pan Mixer from Pemat Mischtechnik GmbH (Freisbach, Germany). Initially, the dry components, i.e., cement and aggregates, were mixed for 120 s. The water was then added and mixed for a further 120 s. After a standing time of 120 s, the mortars were mixed for another 120 s and, after a further standing time of 120 s, the mortars were placed in the appropriate molds. The samples were covered to prevent desiccation and stored at 20 °C for 24 h and then demolded. Subsequently, the substrate mortar slabs were stored under different conditions prior to coating (see Section 2.2.3).

2.2. Methods

2.2.1. Properties of the Substrate Mortars

The consistency of the fresh mortars was characterized by determining the slump flow in accordance with DIN EN 1015-3 [53] (two measurements) and the air void content by means of the pressure method in accordance with DIN EN 1015-7 [54] (one measurement). The flexural and compressive strength of the hardened mortars was determined in accordance with DIN EN 1015-11 [55]. The flexural strength was determined as an average value from three samples and the compressive strength as an average from six samples.

The degree of hydration (DOH) of the cement pastes of mortars M1, M2 and M4 at a certain time (2 d, 7 d, 14 d, 28 d, 56 d and 91 d after casting) was determined from the chemically bound water content, which was determined by measuring the loss of ignition (LOI). Prior to testing, the sealed samples were stored at 20 °C. The reference basis is the maximum water content bound by the cement during complete hydration, $m_{W,\,max}$, which was calculated according to Equation (1), taking into account the composition of the clinker phases of the cements used and their water binding capacity [56]. The degree of hydration could then be calculated according to Equation (2) [56].

$$m_{W,\,max} = x_{C3S} \cdot m_{W,\,C3S} + x_{C2S} \cdot m_{W,\,C2S} + x_{C3A} \cdot m_{W,\,C3A} + x_{C4AF} \cdot m_{W,\,C4AF}, \quad (1)$$

with

$m_{W,\,max}$: maximum water content bound by cement, g.
x_i: proportion of clinker phase i, g/g.
$m_{W,\,i}$: water binding capacity of clinker phase i, g.

$$DOH = \frac{m_{W,\,t}}{m_{W,\,max}} \cdot 100\%, \quad (2)$$

with

DOH: degree of hydration, g.
$m_{W,\,t}$: chemically bound water at time t, g.
$m_{W,\,max}$: maximum water content bound, g.

The composition of the pore solution was also analyzed in the cement pastes of mortars M1, M2, and M4 (The paste of M7 is the same as M1.). Prior to the extraction of the pore solutions, the sealed samples were stored at 20 °C. The pore solutions were obtained at 2 d, 7 d, 14 d, 28 d, 56 d, 91 d and 182 d of hydration by mechanically pressing samples of the pastes using a high-pressure press in the laboratory. The liquid was then filtered, the pH value was determined using a digital laboratory pH meter and the solutions were analyzed by means of ICP-OES, using an ICP-OES ACTIVA-M from HORIBA Europe GmbH (Oberursel, Germany).

2.2.2. Properties of the Coating Systems

The composition of the EP resins and hardeners was determined by means of gas chromatography/mass spectrometry (GC/MS), using an Agilent 8890 GC system and 5977B MSD (Santa Clara, CA, USA). A very small sample of each resin and hardener was dissolved in dichloromethane. After filtration, approximately 1 µL of the solution was analyzed. The GC/MS setup was as follows: (1) fused silica column, length of 30 m, inner diameter of 0.25 mm, and film thickness of 0.25 µm; (2) temperature range of 40–300 °C; (3) heat rate of 10 K/min; (4) column flow (helium) of 1.2 mL/min; and (5) injection volume 1 µL. For the qualification of chemical compounds, Agilent (Santa Clara, CA, USA) MassHunter Version 10.0 software was used.

On the resins and hardeners of the coating systems, the viscosity was determined using a Brookfield DV III-Ultra Viscosimeter from AMETEK GmbH/B.U. Brookfield (Hadamar/Steinbach, Germany). The measurements were carried out with a SC4-29 spindle at a shear rate of 15 s^{-1} and with a sample volume of 13.5 mL. Measurements took place 10 min and 25 min after mixing, respectively. An average value was calculated from three individual measurements.

The degree of curing (DOC) and the glass transition temperatures, T_G, of the EP primers were determined using a differential scanning calorimeter (DSC) Q200 from TA Instruments (Eschborn, Germany). An amount of 20 mg of the primers was put into

aluminum pans and measurements took place on the uncured coating systems directly after mixing (5 min). Further samples were cured at 20 °C in aluminum pans and were measured after 6 h, 12 h, 24 h, 2 d, 3 d, 4 d, 7 d, 14 d, 21 d, 28 d and 56 d, respectively. The temperature range was −40 °C to 300 °C at a heat rate of 10 K/min. From the DSC measurements, the residual enthalpy of the samples at each time point can be obtained and the degree of curing can be calculated from

$$DOC = \left(1 - \frac{\Delta H}{\Delta H_R}\right) \cdot 100\%, \quad (3)$$

with

DOC: degree of curing, %.
ΔH: residual enthalpy, J/g.
ΔH_R: reaction enthalpy, J/g.

Determination of the tensile properties of the coating systems took place in accordance with DIN EN ISO 527-1 [57] on samples of the type 1B. Measurement of tensile strength and elongation took place 4 d, 7 d, 14 d, 28 d and 182 d after preparing the samples and the test speed was set to 2 mm/min. Prior to testing, the samples were stored at 20 °C and 53% RH and under water, respectively. An average value was calculated in each case from five samples.

Water absorption and water diffusion coefficient of the EP systems were determined in accordance with DIN EN ISO 62 Method 1 [58] on samples with the dimensions 60 mm × 60 mm × 1 mm after immersion in water at 23 °C. Prior to the immersion in water, one series of the samples was cured for 28 d and then dried in an oven at 50 °C until the mass of the specimens was constant to within ±0.1 mg/24 h. A second sample series was immersed in water after 4 d of curing and a third series after 28 d of curing, both without prior drying. An average value was calculated in each case from three samples.

Water-vapor transmission properties of the coatings were determined as an average value of three specimens in each case with the wet-cup method according to DIN EN ISO 7783 [59] on circular self-supporting samples with a 100 mm diameter. Prior to testing the samples were conditioned at 20 °C and 53% RH for 28 d. The samples were then sealed to the rims of cups and the assemblies were stored at 20 °C and 53% RH. By means of saturated ammonium dihydrogen phosphate ($NH_4H_2PO_4$) solution, the relative humidity in the cups was maintained at 93%. The mass loss of the assemblies was determined at regular intervals and the rate of flow of water vapor, G, through the specimens was determined so that the water-vapor transmission rate, V, could be calculated (Equation (4) [59]). On one hand, measurements took place on samples of the complete coating systems, i.e., two primer layers (2 × 0.3 mm) plus topcoat (1.5 mm). In this case, the water-vapor diffusion-equivalent air layer thickness, s_d, was calculated (Equation (6) [59]). On the other hand, individual self-supporting sample layers (1 mm) of the primers and the topcoat were measured. The water-vapor resistance factors, μ, could be calculated (Equation (7) [59]):

$$V = \frac{p}{p_0} \cdot \frac{G}{A}, \quad (4)$$

with

V: water-vapor transmission rate, $g/(m^2 \cdot d)$.
G: rate of flow of water vapor, g/h.
A: area of test specimen, m^2.
$\frac{p}{p_0}$: factor to correct V to standard atmospheric pressure.

The atmospheric pressure, p, at the measurement location during the test can be calculated with sufficient accuracy [59]:

$$\frac{p}{p_0} = p_0 - \frac{h}{0.085}, \quad (5)$$

with

p: atmospheric pressure, Pa.
h: height above sea level, m.
p_0: standard atmospheric pressure, Pa, (p_0 = 101,325 Pa).

$$s_d = \frac{\delta_a \cdot \Delta p_V}{V}, \quad (6)$$

with

s_d: water-vapor diffusion-equivalent air layer thickness, m.
δ_a: water-vapor permeation coefficient of air at standard temperature and pressure, g/(m·d·Pa).
Δp_V: difference between the partial water-vapor pressure in the test cup and that in the test enclosure, Pa.

$$\mu = \frac{s_d}{d}, \quad (7)$$

with

μ: water-vapor resistance factor.
s_d: water-vapor diffusion-equivalent air layer thickness, m.
d: dry-film thickness, m.

Leaching tests were carried out by immersion of free test specimens of the primers with the dimensions 60 mm × 60 mm × 1 mm in different test fluids. Three different test fluids were used: (1) deionized water, (2) synthetic pore solution (SPS; 400 mmol/L potassium, 100 mmol/L sodium, saturated with calcium hydroxide, pH = 13.7) similar to the pore solution which was obtained from the substrate mortars (see Section 3.1), and (3) synthetic pore solution (170 mmol/L potassium, 17 mmol/L sodium, saturated with calcium hydroxide, and pH = 13.4), which was based on a pore solution used by Wolff [5]. The samples were stored in the test fluids after 4 d and 35 d of curing and the containers were stored at 20 °C and 30 °C, respectively. After 3 d, 28 d and 56 d of leaching, eluates of the solutions were prepared as follows: (1) approximately 1 mL of the solution was taken from the container; (2) approximately 3 mL of dichloromethane were added; (3) the inhomogeneous mixture was shaken vigorously; (4) the dichloromethane was transferred to another vial; (5) anhydrous sodium sulfate was added to bind any water; and (6) decanting. Approximately 1 µL of each eluate was then analyzed using GC/MS with the same setup as described above.

2.2.3. Composite Test Specimens

For the long-term tests on blistering under different conditions, substrate slabs of the dimensions 300 mm × 300 mm × 60 mm were produced from the mortars described above. After demolding, one part of the specimens was stored at 20 °C/65% RH and the second part was stored under water for 7 weeks. For surface preparation (removal of cement skin and loose material, exposing the aggregate at the surface), the slabs were blasted with slag. For better handling, the slabs were then divided up into smaller test specimens (150 mm × 150 mm × 60 mm), which have proven themselves useful in preliminary works

by the authors. The specimen series was subsequently stored for another week under the following conditions:

1. 20 °C/65% RH (total storage time 8 weeks; designation 20/65).
2. Underwater storage at 20 °C (total storage time 8 weeks; designation H_2O).
3. CO_2-enriched atmosphere at 20 °C (after 7 weeks at 20 °C/65% RH; designation CO_2).
4. Exposition of the surfaces to be coated to a potassium hydroxide solution for 24 h and storage at 20 °C/65% RH until equilibrium moisture content was reached (after 7 weeks at 20 °C/65% RH); (designation as KOH).

The moisture content of the mortars was determined gravimetrically using the drying method, where a sample was weighed and dried in an oven until its weight remained constant. The weight loss corresponds to the amount of water that has evaporated and the moisture content, u_m, could be calculated according to

$$u_m = \frac{m_w - m_{dry}}{m_{dry}} \cdot 100\%, \quad (8)$$

with

u_m: moisture content, %.
m_w: initial mass before drying, g.
m_{dry}: dry mass, g.

The surface tensile strength and the adhesive strength of the coatings to the substrate plates were determined with the pull-off test in accordance with the DAfSTb Guideline for the protection and repair of concrete structures [43]. To obtain a defined test area, a ring groove with a diameter of 50 mm and a depth of approximately 10 mm was sawed into the surface of the (coated) substrate slabs. The area was cleaned and a dolly was applied with polymethyl methacrylate (PMMA) adhesive SILIKAL RI/21 from Silikal GmbH (Mainhausen, Germany). The tensile test was performed using a tensile tester F15D EASY M2000 from Baustoffprüfsysteme Wennigsen GmbH (Wennigsen, Germany) and a constant load increase rate of 100 N/s was applied. An average value was calculated from five individual measurements.

The substrate slabs were coated 8 weeks after manufacturing. The quantities (layer thicknesses) used were based on the consumption values specified in the technical data sheets of the coating materials and corresponded with practical applications. The primers were applied in two layers with a single-layer thickness of 0.3 mm. The transparent topcoat was then applied with a layer thickness of 1.5 mm. The materials were applied with small paint rollers with a curing time of 24 h for each layer. To ensure that comparable quantities were applied, and thus that uniform layer thicknesses were achieved, the coating was applied on a scale. Before coating the side surfaces of composite test specimens were sealed with butyl tape, a polyethylene film and a tear-resistant fabric. After 4 d of resin curing, the specimens were placed into different storage conditions.

In addition to dry-stored reference samples, specimens were placed into footbaths (Figure 2) with different temperatures to investigate blister development with rear moisture penetration. Such temperature differences can occur, for example, through the use of underfloor heating or in parking garages. The storage conditions were as follows:

1. 20 °C/65% RH (dry, reference; designation REF);
2. 20 °C/65% RH with a foot bath of 20 °C (designation FB20);
3. 20 °C/65% RH with a foot bath of 30 °C (designation FB30);
4. 20 °C/65% RH with a foot bath of 10 °C (designation FB10).

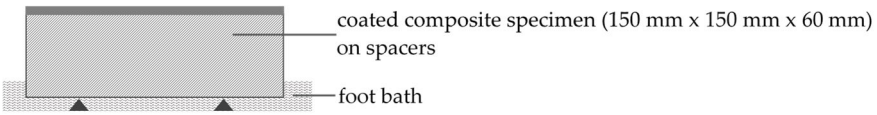

Figure 2. Illustration of foot bath storage.

In storage conditions REF and FB20, three slabs of each combination were stored; in storage conditions FB30 and FB10, one slab of each combination was stored.

After an observation period of 14 months, the specimens with mortars M1, M2 and M4 that were initially stored dry at 20 °C/65% RH (REF) were transferred to a footbath of 20 °C for comparative reasons.

The designation of the composite specimens follows the following scheme: [substrate mortar]_[primer]_[storage before coating]_[storage after coating]. For example, M1_EP2_20/65_FB20 is a specimen of substrate mortar M1 coated with primer EP2 and EP topcoat. The substrate slab was stored at 20 °C/65% RH before coating and placed in 20 °C/65% RH with a foot bath of 20 °C after coating.

Of the composite specimens, high-resolution images were taken at regular intervals to provide insights into the location and timing of blister formation. In the images, the blisters were marked and binary images were produced. The images were processed with Adobe Photoshop Version 26.11.2 from Adobe Inc. (San José, CA, USA) and ImageJ 1.54r (Wayne Rasband and contributors, the National Institutes of Health, Bethesda, MD, USA) [60]. The processing of these images and the differential images produced from them allowed conclusions to be drawn about the growth rate of the blister area and number.

Where possible, any blister fluids were extracted and their organic and inorganic compounds were analyzed by means of GC/MS and ICP-OES, respectively. Sample preparation for GC/MS analysis and setup of GC/MS took place as described above.

The quantitative pore size distribution of the substrate mortars was determined by means of mercury high-pressure porosimetry. Small samples of approximately 10 mm × 10 mm × 10 mm were examined with an AutoPore III-9400 mercury porosimeter from Micromeritics (Norcross, GA, USA). With the porosimeter used, pore radii from approximately 5 nm to 200 µm can be detected.

There are cases in practice where blistering of resin floors occurred without apparent rear moisture penetration. This is where high humidity supply, i.e., vaporous water and possibly condensation, comes to mind. To investigate this circumstance, an experimental setup was developed (Figure 3), where a coated substrate specimen was subjected to different levels of humidity on both sides. On the coated side (upper side), the chamber was equipped with a container of silica gel as desiccant; the humidity was kept at approximately 11% RH. On the uncoated side of the specimen (underside), a water container was placed to keep the humidity in that chamber at 100% RH. The substrate specimens were cast in plastic tubes with a diameter of 126 mm and then cut into disks of 30 mm thickness. After a hydration time of 8 weeks, the substrate disks were coated and equipped with two temperature and humidity sensors in boreholes: one under the coating and one near the uncoated surface. The specimens were then sealed into the test setup and stored at 20 °C. The temperature and also the relative humidity inside the samples were continuously recorded until equalization to approximately 100% RH under the coating was reached. After a certain period of observation for possible blistering, the setup was equipped with a fan-cooled heat sink in order to be able to cool the specimen to under dew point temperature to induce condensation.

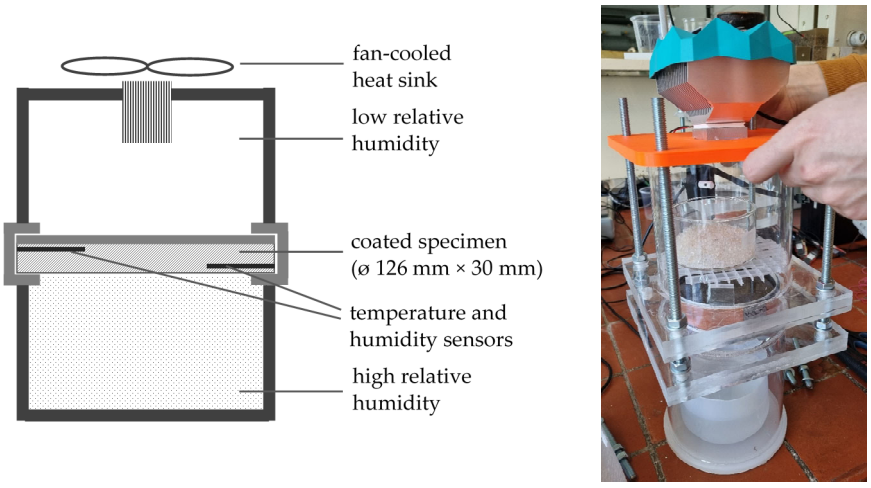

(**a**) (**b**)

Figure 3. (**a**) Illustration and (**b**) photograph of experimental setup with different levels of humidity.

To investigate whether ASR contributed to blister formation, a thin section measuring 48 mm × 35 mm was prepared from a suitable area on the surface of the test specimen of mortar M7 with blistering under the coating. The finished thin sections had a standard thickness of approximately 25 µm with an area of 48 mm × 35 mm. The samples were vacuum-impregnated with a synthetic resin containing a yellow fluorescent dye to improve contrast. The polarizing microscope examinations were performed using a Nikon Eclipse LV 100 ND microscope, and the thin sections were photographed using a Nikon digital camera, Nikon Metrology Europe NV (Leuven, Belgium).

3. Results and Discussion

3.1. Properties of the Substrate Mortars

The results for the fresh mortar tests are shown in Table 7. Due to its lower w/c, mortar M4 had a much lower slump and was therefore more difficult to compact and work with.

Table 7. Fresh mortar properties.

Sample ID	Slump (mm)	Air Void Content (%)	Fresh Bulk Density (kg/m^3)
M1	210	1.8	2250
M2	214	1.9	2260
M4	114	4.9	2260
M7	208	2.1	2240

The properties of the hardened mortars are presented in Table 8. As the cement paste of M7 has the same composition as that of M1, the DOH of M7 was not determined separately.

The measured pH values and compositions of the pore solutions of the pastes of M1, M2, and M4 are presented in Table 9. The paste of M7 has not been examined separately, as it has the same composition as M1. The composition of the SPS for the leaching tests is based on the ratio of the concentrations of sodium and potassium Na/K, which is approximately 1/4.

Table 8. Hardened mortar properties.

Sample ID	Compressive Strength (28 d) (N/mm^2)	Flexural Strength (28 d) (N/mm^2)	Bulk Density (28 d) (kg/m^3)	DOH Cement Pastes (91 d) (%)
M1	37.8	6.0	2100	83.8
M2	31.5	5.7	2100	77.8
M4	41.1	6.2	2200	70.4
M7	47.9	6.4	2300	n.d. *

* n.d.—not determined.

Table 9. Measured pH and concentrations in pore solutions of cement pastes M1, M2, and M4.

Sample ID	Time (d)	pH (-)	Na	K	Ca	Si	S	Cl
					(mmol/L)			
M1	2	13.74	83	391	1.8	0.45	2.2	8.7
	7	13.75	115	467	1.4	0.66	4.8	n.d. *
	14	13.72	125	497	1.3	0.90	5.8	n.d.
	28	13.72	134	526	1.4	0.56	7.8	4.3
	56	13.72	148	577	1.2	0.77	12.3	5.3
	90	13.81	144	549	1.0	1.06	12.6	6.2
	180	13.74	148	549	1.0	1.07	15.4	5.4
M2	2	13.48	41	190	4.0	0.22	0.4	2.4
	7	13.43	54	222	2.9	0.43	0.5	n.d.
	14	13.44	63	244	2.2	0.78	0.9	n.d.
	28	13.50	65	248	2.3	0.49	1.2	n.d.
	56	13.49	72	257	1.6	0.73	1.7	0.4
	90	13.56	74	278	1.9	0.48	2.1	0.4
	180	13.49	77	274	1.3	0.82	2.9	0.5
M4	2	13.53	60	280	1.6	0.89	1.4	2.0
	7	13.58	81	355	1.7	1.24	2.3	n.d.
	14	13.60	86	358	1.6	0.95	3.5	n.d.
	28	13.64	88	373	1.5	0.95	4.2	0.5
	56	13.58	93	383	1.5	0.79	5.2	0.5
	90	13.66	103	419	1.0	1.96	6.9	0.5
	180	13.59	146	403	0.7	3.14	7.9	0.4

* n.d.—not determined.

The water absorption coefficients, w, of the mortars M1, M2, and M4 were determined by the project partner (see "Funding" Section) and are shown in Table 10.

Table 10. Water absorption coefficients of mortars M1, M2, and M4.

	M1	M2	M4
Water absorption coefficient ($kg/(m^2 \cdot h^{0.5})$)	1.57 (±0.02)	2.07 (±0.07)	1.19 (±0.01)

3.2. Properties of the Coating Systems

When examining the composition of the EP systems by means of GC/MS, bisphenol A diglycidyl ether was found to be the main component of the resins. C12–C14 alkyl glycidyl ether was also detected, particularly in the primers, where it is used to reduce viscosity. In the EP hardeners, various amines and diamines, such as *m*-xylylenediamine, isophorone diamine, bisphenol A-epichlorohydrin–isophoronediamine copolymer, polyoxypropylene-diamine, and trimethylhexamethylenediamine were detected. Furthermore, in the hardener of EP1, benzyl alcohol was detected, which typically serves as a plasticizer or diluent. These investigations served as the basis for the leaching tests. The results obtained here can be used to identify any components that may have been leached out of the cured EP systems.

In Table 11, the viscosity parameters of the uncured EP systems are summarized. As expected for resin systems used for coatings, the viscosities of both the primers and the topcoat are relatively high, although the viscosities of EP1 and EP2 differ by approximately 50%. Generally, the viscosity parameters match the values given in the datasheets.

Table 11. Viscosity parameters of uncured coating systems 10 min and 25 min after mixing, and from datasheets.

Sample ID	Viscosity (10 min) (mPa·s)	Viscosity (25 min) (mPa·s)	Viscosity (Datasheet) (mPa·s)
EP1	842	1308	800
EP2	464	653	500
EP topcoat	1084	1454	1000

The evaluation of the DSC measurements of the EP primers shows typical parabolic curves for residual enthalpy over curing time (Figure 4a). The degrees of curing were calculated with Equation (3) and are displayed in Figure 4b together with the development of the glass transition temperature over curing time. When measuring mostly cured EP, DSC often cannot detect any significant residual enthalpy, as only a few bonds are still being formed. However, as the formation of these bonds further increases the network density, the glass transition temperature, T_G, continues to rise (Figure 4c). The increase in glass transition temperature indicates further curing, even if no residual enthalpy can be detected [61–63].

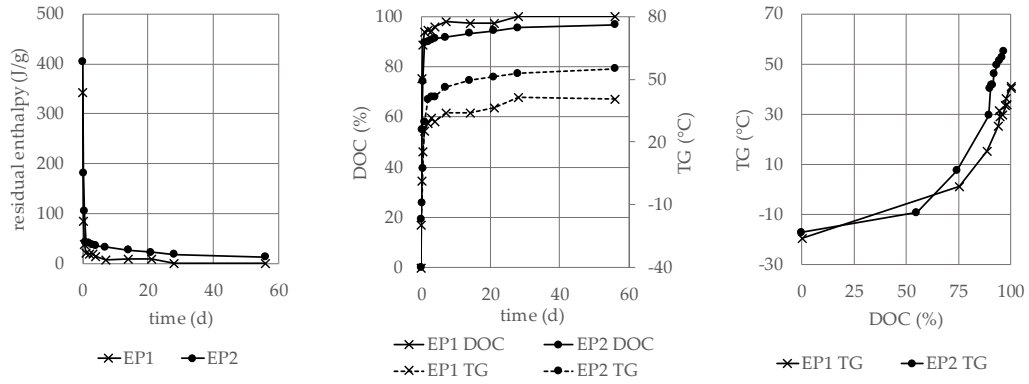

(**a**) (**b**) (**c**)

Figure 4. Development over time of (**a**) residual enthalpy and (**b**) DOC and T_G of the EP primers after different curing times; (**c**) T_G from DSC measurements over DOC from residual enthalpy measurements for different curing states.

The tensile properties of the EP systems after different times of curing and storage at 20 °C and 53% RH and under water, respectively, are presented in Figure 5. Water absorption, i.e., the storage of water molecules in the polymer network, can act as a plasticizer, which can lead to a reduction in the mechanical properties of the resin. This effect is reversible when the material dries out, e.g., [64,65]. In this study, water storage only had a significant influence on the development of tensile strength in EP1, where a decrease could be observed.

Figure 6 shows the water absorption of the EP resins. All the systems initially show a linear increase according to Fick's 1st law. While EP2 and EP topcoat subsequently show a slight further increase in mass, EP1 shows a decrease in mass. This is due to the leaching of benzyl alcohol from the polymer [66]. As expected, the pre-dried samples show the highest water absorption, while the samples that were allowed to cure for 28 days prior

to immersion show the lowest water absorption. Water diffusion coefficients, D, were derived for the samples without prior drying (Table 12). The diffusion coefficients of samples that cured for 28 d before immersion are lower than those for samples that cured for only 4 d. Literature values vary considerably (e.g., $D = 0.54 \cdot 10^{-11}$ cm^2/s at 40 °C [67], $D = 2.0 \cdot 10^{-8}$ cm^2/s [66], and $D = 0.53 \cdot 10^{-9}$ cm^2/s at 20 °C [68]) as the water diffusion coefficient depends on temperature, cross-linking density and additives.

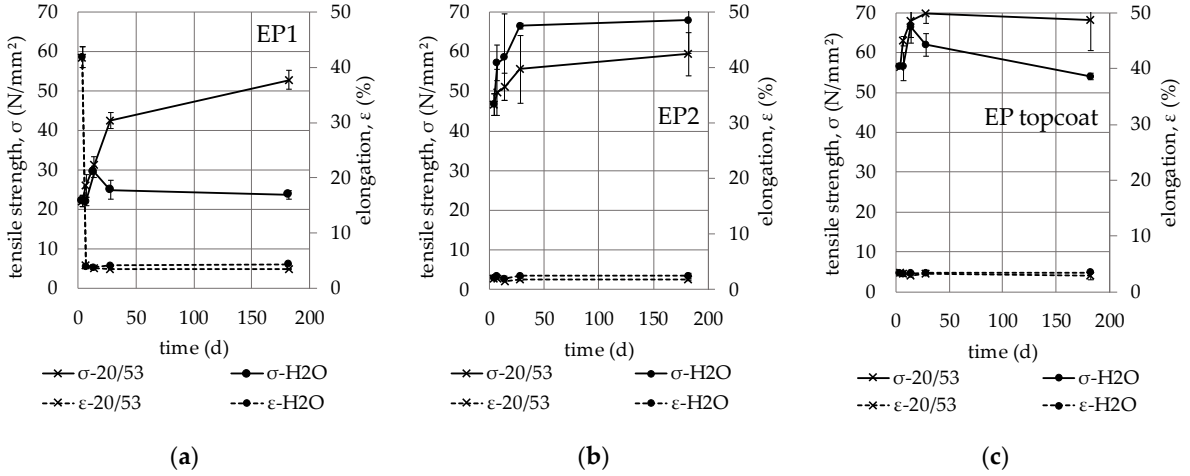

Figure 5. Development over time of tensile strength (solid line) and elongation at tensile strength (dashed line) of (**a**) EP1, (**b**) EP2 and (**c**) EP topcoat after storage at 20 °C and 53% RH (cross marking) and under water (dot marking).

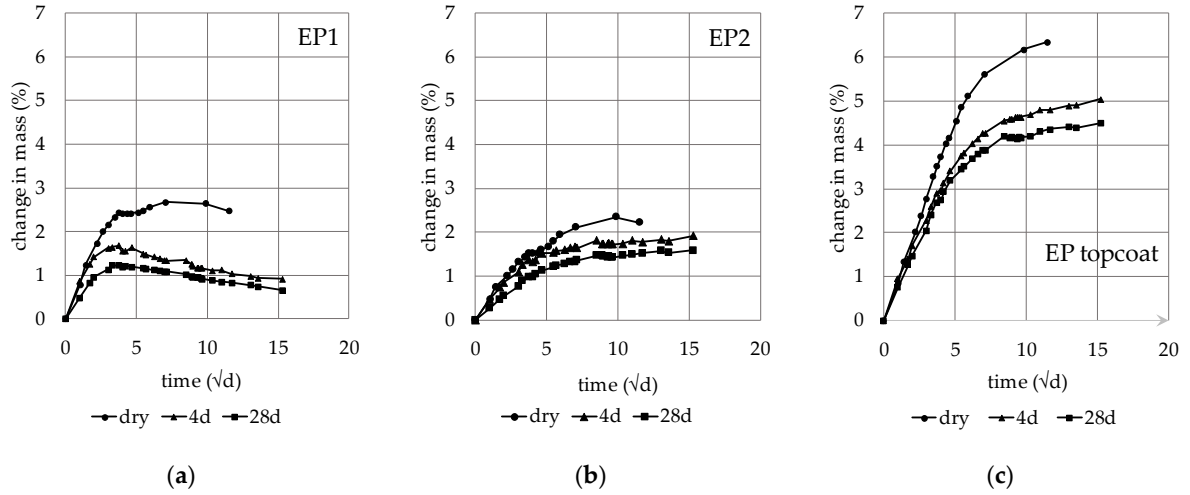

Figure 6. Water absorption of (**a**) EP1, (**b**) EP2 and (**c**) EP topcoat, immersion in water after prior drying (dry), after 4 d of curing and after 28 d of curing.

In Table 13, the determined water-vapor resistance factors, μ, for individual EP resins are shown. From these factors, the water-vapor diffusion-equivalent air layer thicknesses, s_d, for the complete coating systems were calculated with Equation (7) and compared to the determined values. The calculation of s_d from the individual layers of the EP primers and topcoat determined μ, generally resulted in higher s_d-values than the determination of s_d on the complete coating systems. The reason for this is most likely the difficulty of producing a uniform layer thickness of 0.3 mm for the primers. This problem will also occur in practice. Generally, the determined s_d-values are close to the limit value $s_d < 5$ m, which is considered "permeable to water vapor"; $s_d > 50$ m is considered "not permeable to water vapor" [69].

Table 12. Water diffusion coefficients, D, of coating systems, immersion after 4 d and 28 d of curing.

Sample ID	D, Immersion After 4 d ($\cdot 10^{-10}$ cm^2/s)	D, Immersion After 28 d ($\cdot 10^{-10}$ cm^2/s)
EP1	46.1	37.3
EP2	7.0	5.6
EP topcoat	4.8	5.6

Table 13. Water-vapor resistance factors, μ, for individual EP resins and water-vapor diffusion-equivalent air layer thickness, s_d, for complete coating systems, measured and calculated in μ.

Sample ID	μ (-)	Sample ID	s_d Determined (m)	s_d Calculated (m)
EP1	4060	EP1 + EP topcoat	5.3	19.8
EP2	23,450	EP2 + EP topcoat	5.7	31.5
EP topcoat	17,400	-	-	-

In the leaching tests, benzyl alcohol was the only organic component that could be detected in all three test fluids with EP1 samples; no leached components could be detected in the storage fluids with EP2 samples (Figure 7). Furthermore, no influence from the test fluids, the storage temperature or the storage time could be detected: even at 30 °C and after longer storage, no other organic compound could be found than benzyl alcohol in samples with EP1. It can therefore be assumed that, at least in these investigations, no other components from the coating materials, especially EP2, can be responsible for blistering.

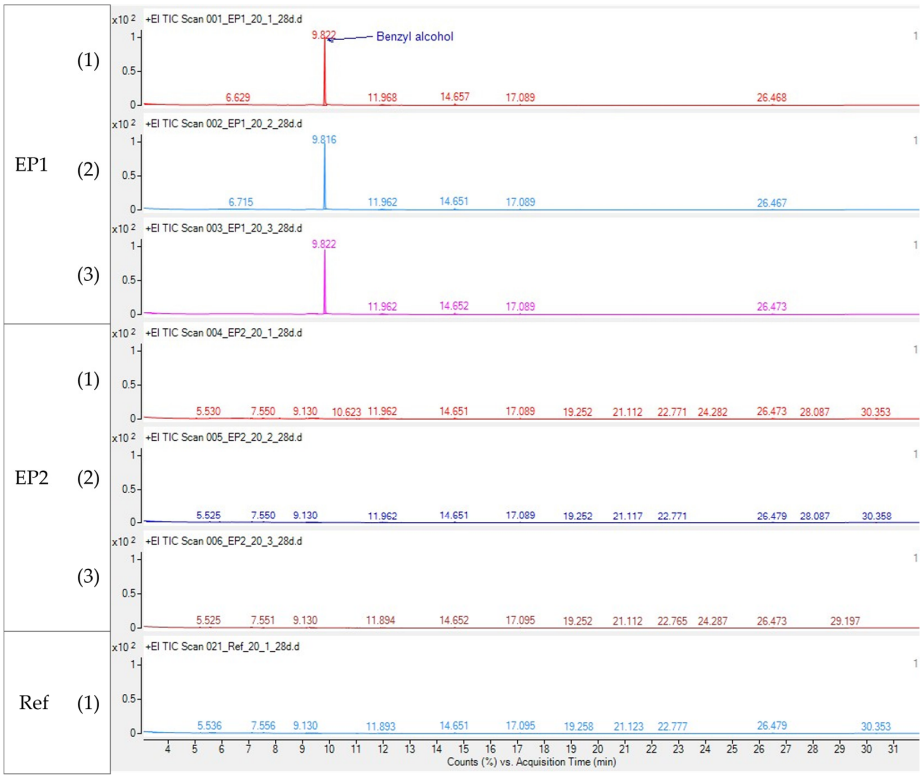

Figure 7. Gas chromatograms of eluates from leaching solutions with EP1 and EP2 in (1) deionized water, (2) synthetic pore solution (400 mmol/L potassium, 100 mmol/L sodium, saturated with calcium hydroxide, pH = 13.7), and (3) synthetic pore solution (170 mmol/L of potassium, 17 mmol/L of sodium, saturated with calcium hydroxide, pH = 13.4), stored at 20 °C, samples taken after 28 d of leaching.

3.3. Composite Test Specimens

The moisture content of the mortars during coating is displayed in Table 14. Mortar M4 has the lowest moisture content, which can be explained by its lower w/c ratio of 0.4 compared to 0.55 in M1, M2, and M7.

Table 14. Moisture content of mortars during coating.

	Storage Before Coating	M1	M2	M4	M7
Moisture content (wt. %)	20/65	5.7	4.1	3.6	5.5
	H_2O	7.1	7.7	5.5	6.7

The surface tensile strength of the mortars and the adhesive strength of the primers on the mortars are shown in Table 15. Generally, the surface tensile strength of all mortars can be considered as very high (mean value > 1.5 N/mm^2 [43]), which is a prerequisite for a durable bond of coating and concrete. The adhesive strength of the coating systems on all mortars also meets the minimum requirement of 1.5 N/mm^2 (mean value) [43]. Overall, EP1 tends to have higher adhesive strength than EP2, apart from on specimens that have been stored under water before coating. The adhesive strength of EP2 is highest on slabs that have been stored under water before coating and lowest on slabs that have been stored in a CO_2-enriched atmosphere at 20 °C. For EP2, there is no significant influence from mortar composition visible.

Table 15. Surface tensile strength of mortars M1, M2, M4, and M7, and adhesive strength of EP1 and EP2 on M1, M2, M4, and M7 after different storage periods before coating.

	Storage Before Coating	Primer	M1	M2	M4	M7
Surface tensile strength (N/mm^2)	-	-	3.1 (±0.3)	3.6 (±0.6)	3.6 (±0.3)	3.6 (±0.3)
Adhesive strength (N/mm^2)	20/65	EP1	2.8 (±0.3)	2.7 (±0.2)	3.3 (±0.1)	3.0 (±0.5)
		EP2	3.1 (±0.4)	3.1 (±0.3)	2.8 (±0.2)	3.0 (±0.3)
	H_2O	EP1	2.8 (±0.5)	3.2 (±0.2)	3.6 (±0.3)	n.d.
		EP2	3.6 (±0.2)	3.8 (±0.2)	4.0 (±0.1)	3.7 (±1.4)
	CO_2	EP1	2.7 (±0.7)	3.0 (±0.2)	3.5 (±0.3)	3.6 (±0.2)
		EP2	2.5 (±0.4)	2.3 (±0.2)	2.9 (±0.5)	3.1 (±0.4)
	KOH	EP1	3.0 (±0.3)	3.0 (±0.3)	3.2 (±0.2)	3.3 (±0.3)
		EP2	2.8 (±0.3)	2.7 (±0.5)	3.2 (±0.3)	3.6 (±0.3)

3.4. Long-Term Investigations

In the long-term studies, it was observed whether and when blisters would be formed on the individual slabs. All the blisters that occurred in these investigations formed in the interface between the coating and the substrate mortar. Figure 8 shows an overview of the blistering of the two coating systems on the mortars at different storage conditions, before and after coating, with the placement of the composite test specimens into the footbath 4 d after coating. It can be observed that, apart from one exception, without backward moisture penetration, no blistering occurred. A higher water content, i.e., underwater storage prior to coating, had a positive effect in terms of less blistering. Furthermore, blistering occurred regardless of the benzyl alcohol content in the primers. Additionally, the substrate mortar with a lower w/c = 0.4 tended to have less blistering.

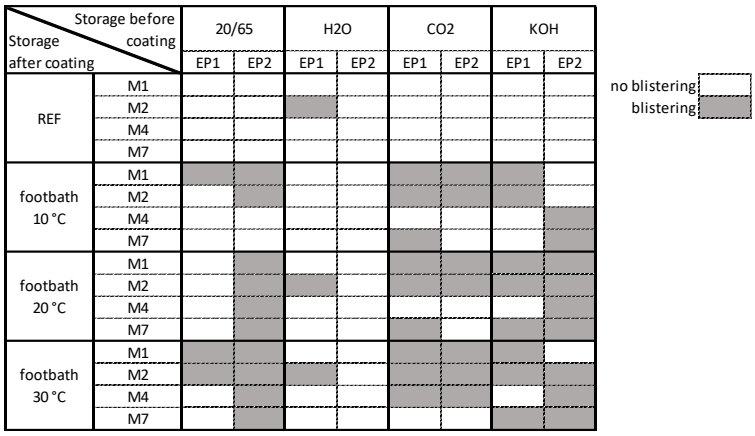

Figure 8. Overview of blistering of EP1 and EP2 on M1, M2, M4, and M7 with different storage conditions before and after coating; observation period 18 months.

After an observation period of 14 months, the specimens M1, M2, and M4 that were initially stored dry at 20 °C/65% RH (REF) were transferred to FB20 and monitored for blistering that occurred (Figure 9). Once again, it was observed that no blistering occurred in samples that were stored under water prior to coating. The same applies to samples with KOH storage before coating. It is assumed here that exposure to KOH solution increased the moisture content in the substrate, thus producing the same positive effect as in the samples stored under water. Furthermore, no blistering occurred in samples with EP1, thus disproving statements in the literature that benzyl alcohol in EP coatings almost automatically leads to blistering.

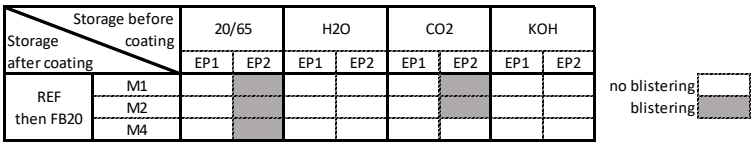

Figure 9. Overview of blistering of EP1 and EP2 on M1, M2, and M4 in FB20 after initial 14 months of dry storage (REF); observation period 12 months in FB20.

Figure 10 shows an example of images of blistering at different times of storage in FB20 and a corresponding binary image that was used to analyze the number of blisters and the blister area ratio.

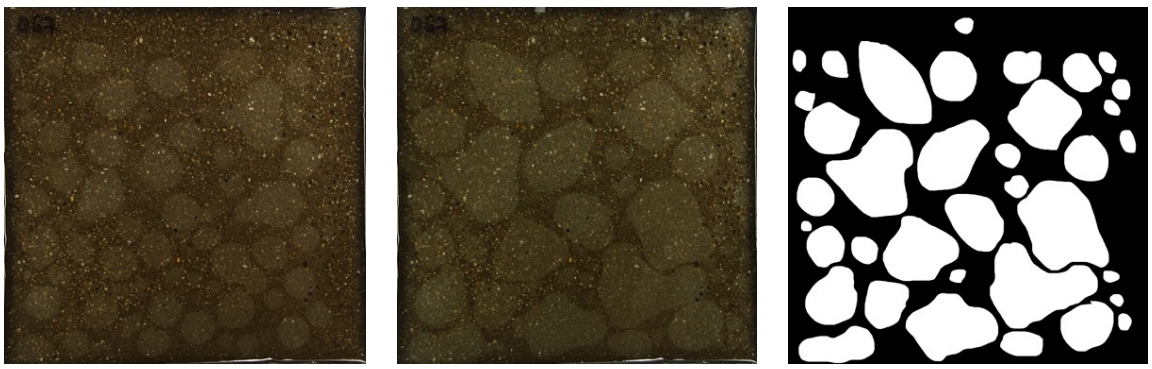

(**a**) (**b**) (**c**)

Figure 10. Image of blistering of M2_EP2_20/65_FB20 after (**a**) 34 d and (**b**) 111 d of storage in FB20; (**c**) binary image of (**b**); edge length of images corresponds to 150 mm.

In Figure 11a, the number of blisters and the corresponding blister area ratio of EP2 on the different mortars for an observation period of 23 weeks are displayed. All the specimens were placed in 20/65 prior to coating and in FB30 4 d after coating. On all mortars, blistering starts within approximately four weeks after placement in the footbath. On M1, the number of blisters increases over the entire observation period. However, the blister diameters are only small (approximately 2 to 10 mm) and the blister area ratio is also small. The blisters on M2, on the other hand, have very large diameters (approximately 8 mm in the beginning to >30 mm at the end of the observation period) and the blisters merge, which is represented by the decreasing number of blisters. On M4, blisters form over a period of approximately three months; individual blisters with similar diameters (approximately 8 to 10 mm) form and they grow only slowly. On M7, individual blisters with a diameter of approximately 5 mm form with a very small blister area ratio. Within this observation period, there is no evidence for blistering caused by ASR. The largest blister area ratio was found on M2 and could similarly be observed with both primers and all footbath temperatures.

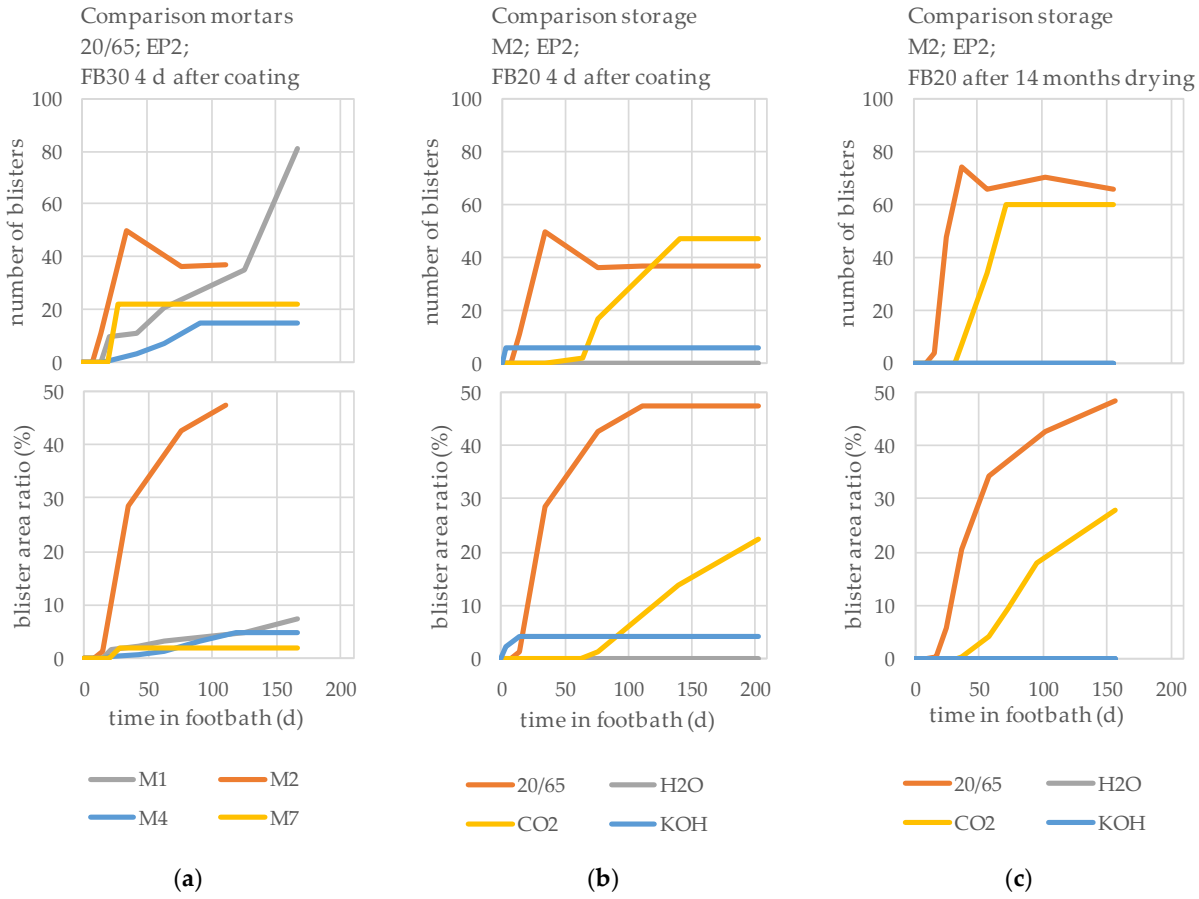

Figure 11. Comparison of number of blisters and blister area ratio of (**a**) all substrate mortars, (**b**) storage conditions before coating and placing in FB20 4 d after coating, and (**c**) storage conditions before coating and placing in FB20 14 months of drying after coating.

When looking at the reasons for the pronounced blister formation on M2, only the higher water absorption coefficient of M2, compared to M1 and M4, could be identified from the substrate properties as having most likely a particularly large influence on blister formation. No other indications from the fresh and hardened mortar properties or the surface tensile strength (see above), and even the evaluation of the pore size analysis (see below), could yield any further clues.

In Figure 11b,c, the blistering of EP2 on M2 is compared with regard to different storage conditions before coating and with samples placed into FB20 4 d after coating and after 14 months of dry storage after coating (REF, see Section 2.2.3). In samples that were stored at 20 °C/65% RH prior to coating (20/65), the blisters formed within approximately four weeks after placing in FB20, with larger diameters of approximately 10 to 20 mm in samples that were placed in FB20 after coating and smaller diameters of approximately 2 to 8 mm in samples that were placed in FB20 after dry storage. In both cases, the blisters merge and blister area ratios of up to almost 50% are reached. For the samples that were stored in a CO_2-enriched atmosphere at 20 °C before coating (CO_2), a significant difference in the time frame of blister formation can be observed. In specimens that were stored in FB20 after coating, blisters (diameter of approximately 2 to 5 mm) formed within approximately 5 months, whereas this time period in samples that were placed in FB20 after 14 months of drying was only approximately 2.5 months, and more blisters formed. Furthermore, the blisters grew faster (to a diameter of max. 20 mm) in the dry stored samples. An influence of carbonation on blister formation can be observed in terms of a later onset of blistering and smaller blister area ratios. For both 20/65 and CO_2 storage before coating, the blister area ratio keeps growing until the end of the observation period and beyond, especially in the dry stored samples. This confirms statements in the literature that an increased likelihood of blister formation increases with concrete that has previously dried out and then been subjected to rear moisture penetration [25]. Underwater storage before coating (H_2O) has a positive effect on both sample series. In the samples that were placed in FB20 4 d after coating, as well as in samples that were stored dry for 14 months after coating, no blistering occurred.

In Figure 12a,b, the blistering of the two coating systems with primers EP1 and EP2 on M2 is compared with regard to the storage conditions prior to coating. In samples that were stored at 20 °C/65% RH prior to coating (20/65), blisters formed within approximately 2 weeks of storage in FB30. In samples with EP1, blisters with larger diameters of up to 30 mm formed and in the samples with EP2, more blisters with slightly smaller diameters of approximately 2 to 15 mm formed. With both coating systems, large blister area ratios are reached with approximately 65% for EP1 and 50% for EP2. This similar blistering behavior of EP1 with benzyl alcohol and EP2 without benzyl alcohol contradicts many statements in the literature that reactive solvents, and benzyl alcohol in particular, have a negative effect and that the omission of the latter can prevent blister formation [9–12]. For the samples that were stored in a CO_2-enriched atmosphere at 20 °C before coating (CO_2), a significant difference in blister formation could be observed for EP1 and EP2. In samples with EP1, individual large blisters (diameter approximately 25 mm) were formed within 2 weeks of storage in FB30, whereas blistering in samples with EP2 started later (3 weeks) and smaller blisters (diameter of ca. 8 mm) formed over a period of approximately 2 months. In samples that were stored under water before coating (H_2O) with EP1, blisters formed within 3 d of placing in FB30. However, in this case, there was no bulging of the blisters.

In Figure 12c, the number of blisters and the blister area ratio of EP2 on M7 after different storage conditions before coating are shown. Blistering starts within approximately 3 weeks of storage in the footbath, similar to M1. Initially, individual blisters with similar diameters form and grow slowly. After about 5 to 6 months, blistering begins again, which is particularly pronounced in samples pretreated with KOH. This subsequent blistering also occurs in samples that have been stored under water before coating. It can be assumed that blistering in this case is caused in particular by ASR, which is known to occur after a certain period of storage. This is confirmed by the thin section examination, in which ASR gel was found in the area of the blisters (Figure 13a).

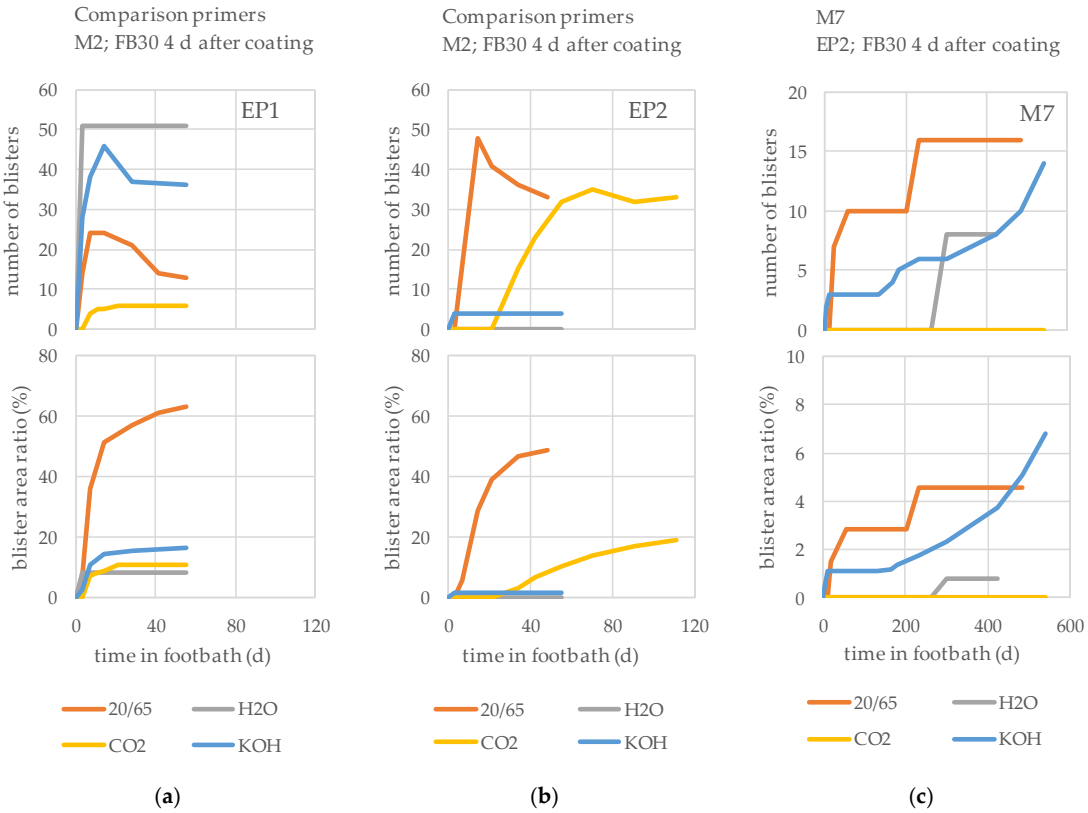

Figure 12. Comparison of number of blisters and blister area ratio of (**a**) EP1 and (**b**) EP2 after different storage conditions before coating, and (**c**) number of blisters and blister area ratio of EP2 on M7 after different storage conditions before coating.

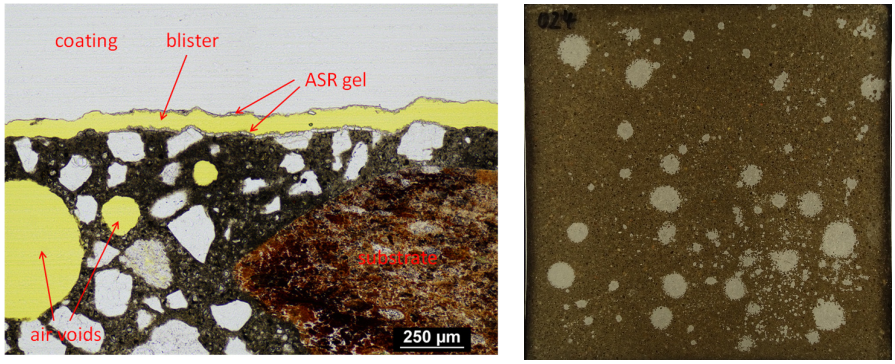

Figure 13. (**a**) Thin section of blistering on M7_EP1_20/65_FB30 with ASR gel in the area of the blister; (**b**) image of blistering without bulging M2_EP1_H2O_FB30; edge length of slab = 150 mm.

Another phenomenon was observed in which blisters formed without bulging. This could be observed in all the mortars and in all the storage conditions before and after coating without any system. These blisters did not contain any liquid and could only be detected due to the use of a transparent topcoat (Figure 13b). It is assumed that in practice, blisters of this kind also occur and cannot be detected, as most coating systems contain fillers or pigments. Therefore, it is highly likely that many cases of blister formation or delamination go undetected.

From these results, it can be derived that blistering of EP coatings on concrete depends especially on the treatment of the substrate material before coating, i.e., dry storage (here,

20/65 and CO_2) in particular can lead to severe blister formation; with higher moisture contents, blistering can be avoided.

Only from individual blisters of M2_EP1_20/65_FB30 and M2_EP2_CO2_FB20, very little fluid could be extracted and examined. The results of ICP-OES measurements are displayed in Table 16, and the results of GC/MS examination are shown in Figure 14. As there was not enough fluid, examination of the pH value could not be carried out with a pH meter but was conducted with litmus paper directly on the composite test specimen. The concentrations of potassium and sodium of the blister fluid are very similar to those in the pore solution of M2. As in the leaching tests, the only organic compound identified in the blister fluids was benzyl alcohol. As there could not have been detected any other (unreacted) components of EP1 in the blister fluids, it can be assumed that the coating on the composite test specimens was fully cured. From composite test specimens with EP2, no blister fluid could be obtained.

Table 16. Measured concentrations in blister fluids.

Sample ID	Time (d)	pH (-)	Na	K	Ca	Si	S	Cl
			(mmol/L)					
M2_EP1_20/65_FB30	200	>13	80	230	0.2	4.2	10.2	1.3
M2_EP1_CO2_FB20	200	>13	95	307	0.2	22.1	30.5	1.8

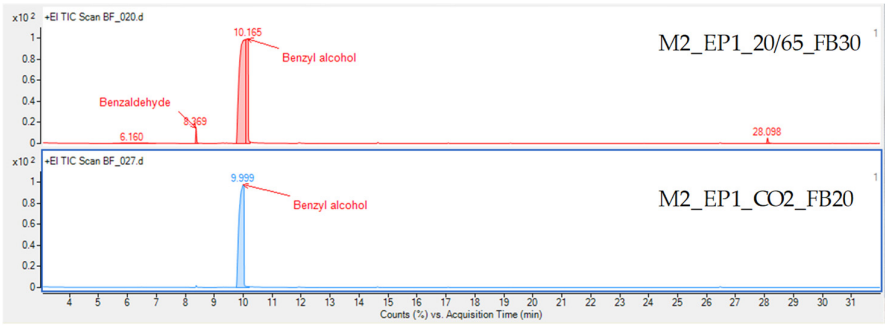

Figure 14. Gas chromatograms of blister fluids taken from M2_EP1_20/65_FB30 and M2_EP2_CO2_FB20.

Quantitative pore size distribution of the substrate mortars was determined on composite specimens with and without blistering. Samples were taken from directly under the coating (approximately 10 mm) and from the center of the substrate slabs. For quantitative comparison, the pore size ranges were classified according to Romberg [70] with gel pore radii ranging from 1 to 10 nm and capillary pore radii from 10 nm to 100 µm. The following figures (Figures 15–17) show the pore size distribution and classification of pore size ranges of mortars M1, M2, and M4 taken from different storage locations before and after coating. Generally, M1, M2, and M4 had a very similar distribution of gel and capillary pores, though the distribution of gel pores of M2 fluctuated slightly more than that of M1 and M4. However, these results indicate no obvious influence on blistering/no blistering from the pore size distribution. None of the mortars clearly shows whether blistering occurs at higher or lower levels of capillary pores. Therefore, in this study, no influence from the type of cement or w/c on blister formation could be derived.

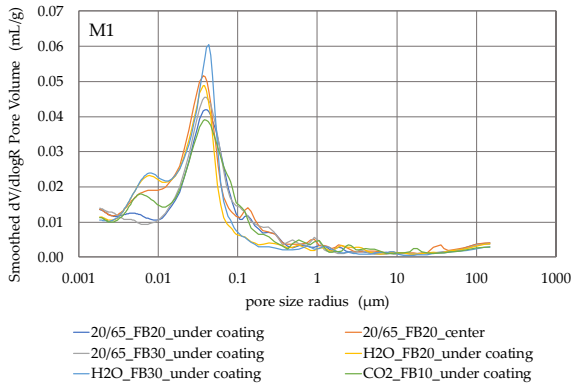

(**a**)

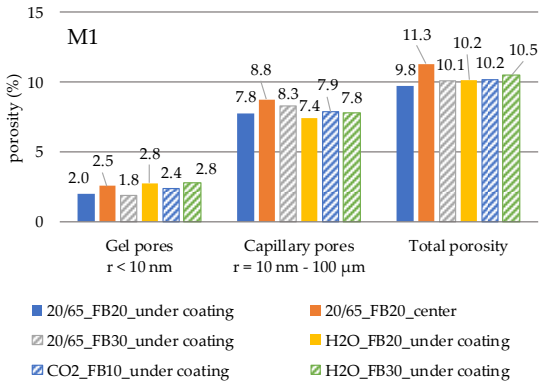

(**b**)

Figure 15. (**a**) Pore size distribution of samples taken from composite specimens M1 and (**b**) corresponding pore size ranges according to Romberg [70] with solid columns where no blistering occurred and hatched columns where blistering occurred.

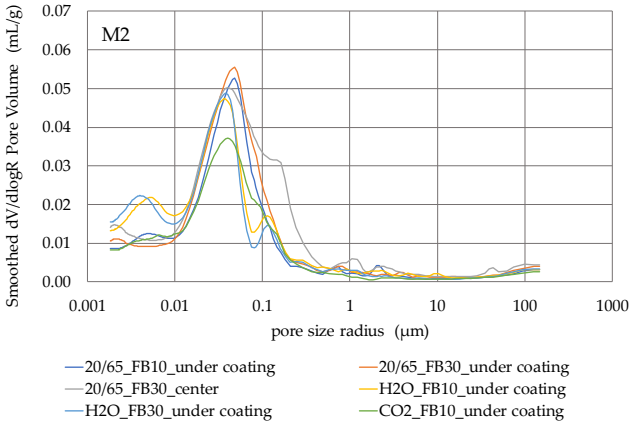

(**a**)

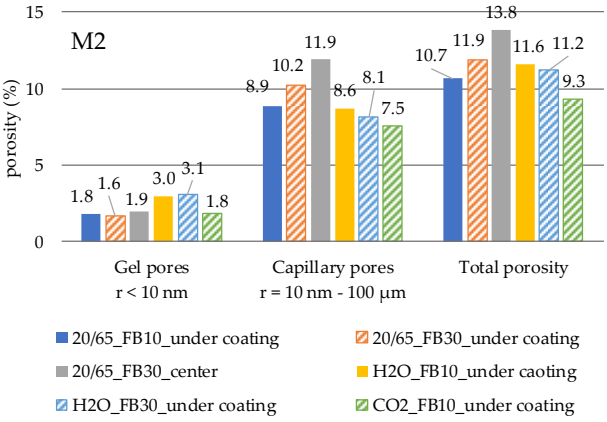

(**b**)

Figure 16. (**a**) Pore size distribution of samples taken from composite specimens M2 and (**b**) corresponding pore size ranges according to Romberg [70] with solid columns where no blistering occurred and hatched columns where blistering occurred.

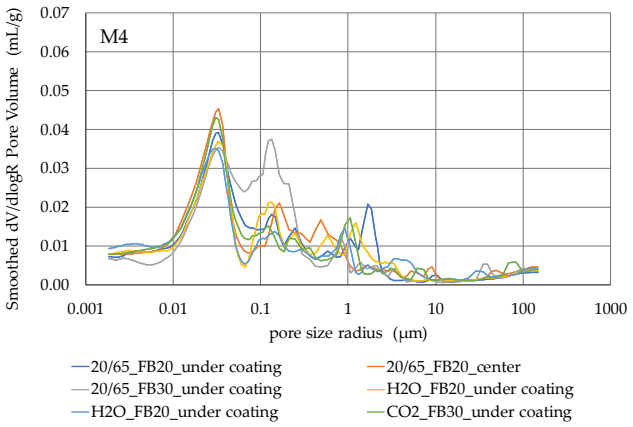

(**a**)

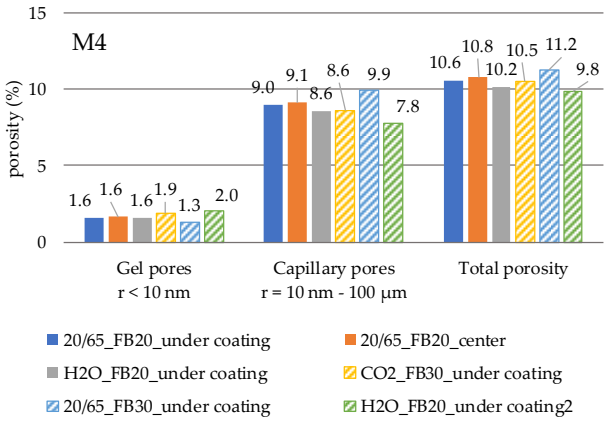

(**b**)

Figure 17. (**a**) Pore size distribution of samples taken from composite specimens M4 and (**b**) corresponding pore size ranges according to Romberg [70] with solid columns where no blistering occurred and hatched columns where blistering occurred.

In the test setup with different levels of humidity on the coated and uncoated sides, samples with EP1 on mortar M2 were investigated. After the sealing, equalization to 95% within the substrate directly under the coating took approximately 35 d. The samples were then observed for 6 months and no blistering could be detected within this period (Figure 18b). The setup was then equipped with the fan-cooled heat sink and the (dry) chamber on the coated side of the specimen was cooled to under the dew point temperature of 21.2 °C. Condensation occurred inside and on the underside of the specimens (Figure 18a). Thus, fluid water was available and blistering occurred within approximately 3 months of cooling (Figure 18c). From these results, it can be concluded that condensation in substrate materials can provide sufficient amounts of water to cause blistering in resin coatings.

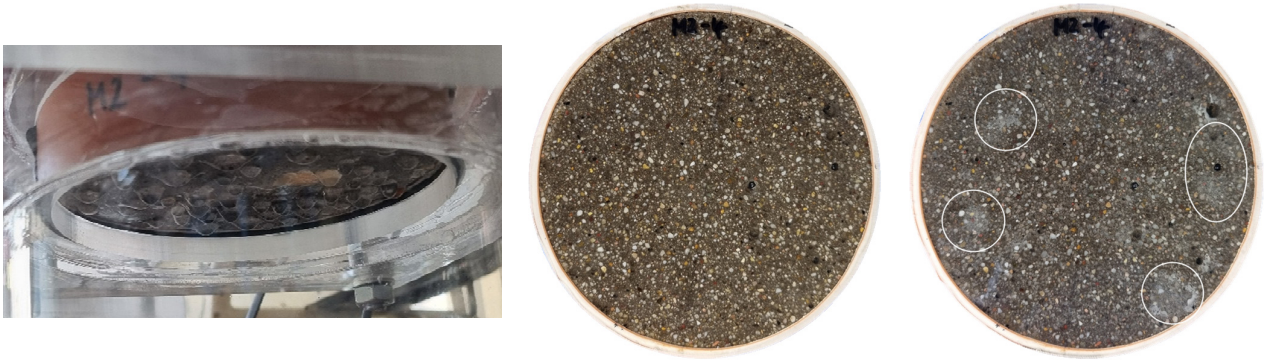

(**a**) (**b**) (**c**)

Figure 18. (**a**) Condensation on the underside of composite test specimen EP1 on M2 in test setup with different levels of humidity on the coated and uncoated side; (**b**) composite test specimen (ø 126 mm) with 95% RH in boreholes before cooling; (**c**) composite test specimen (ø 126 mm) after approximately 3 months, with blisters clearly visible in the indicated areas.

4. Conclusions

From the results presented and discussed above, the following conclusions can be drawn with regard to blistering of EP resin coatings on concrete:

1. Blistering of EP coatings on concrete depends especially on the treatment of the substrate material before coating, i.e., dry storage (here 20/65 and CO_2) in particular leads to severe blister formation, when rear moisture penetration occurs.
2. In samples with lower moisture contents in the substrate, rear moisture penetration almost always leads to blistering. Avoidance of rear moisture penetration in practice can help to prevent blistering of resin coatings on concrete.
3. Higher moisture contents in the substrate prior to coating have a positive effect in terms of less to no blistering when rear moisture penetration occurs shortly after coating.
4. Underwater storage before coating can also prevent blistering, when rear water penetration occurs after a longer period of drying after coating. In practice, this means that adequate curing of the cementitious substrate material can help to avoid blistering of resin coatings on (young) concrete.
5. The EP systems containing benzyl alcohol are not automatically vulnerable to blister formation: in samples, where rear moisture penetration was applied after 14 months of dry storage, no blistering occurred with EP containing benzyl alcohol.
6. In some cases, blistering occurred without bulging. This could only be detected due to the application of a transparent topcoat. It is therefore assumed that, in practice, some cases of blister formation and/or delamination go undetected, as in most cases the coating systems contain fillers or pigments.

7. The composition of the mortar has an influence on blister formation in that a higher water absorption coefficient leads to more blister formation.
8. Condensation in samples with high relative humidity in the pore system provides a sufficient amount of water to cause blistering.
9. ASR contributes to blister formation.
10. No other organic compounds than the benzyl alcohol (where applicable) were detected in leaching tests in deionized water and synthetic pore solutions at different temperatures.
11. Benzyl alcohol was the only organic compound found in blister fluid from EP containing benzyl alcohol.
12. The inorganic composition of the blister fluid from EP containing benzyl alcohol is very similar to the pore solution of the corresponding mortar.

Limitations

In this study, mortars were used as substitute materials for the concrete used in practice. These are more homogeneous, and smaller test specimens can be produced. Since the work was conducted as part of a collaborative project, the requirements of the project partners also had to be taken into account; in their experiments, only test specimens of small dimensions could be used. Furthermore, in concretes, in addition to a larger maximum aggregate size, admixtures and additives are typically used, and their potential effects on blister formation should explicitly be excluded in this study. Based on the findings obtained here, it is not expected that the use of a larger maximum aggregate size would have yielded fundamentally different results.

The time periods and points for the formation of blisters specified in this study may, of course, vary for other laboratory tests with substrate samples of different dimensions, as moisture transport and also the residual moisture present in the substrate depend, amongst others, on the thickness of the substrate (e.g., [39,71]). The same applies in practice, as concrete components to be coated are usually thicker than 60 mm. The influences on blistering of reactive resin coatings on concrete are highly complex. Due to the wide variety of coated structures (e.g., the composition and thickness of the concrete, its moisture content, the material of the coating system, the layer structure, the use of solvents, as well as external factors, such as surface treatment, temperature, and the timing of rear moisture penetration—to name just a few factors), the timing and the range of blister formation in practice will inevitably differ from that observed in this study. However, this does not affect the study's main findings.

Author Contributions: Conceptualization, F.V.; methodology, F.V. and A.O.; validation, F.V. and A.O.; formal analysis, F.V.; investigation, F.V.; resources, A.O.; data curation, F.V.; writing—original draft preparation, F.V.; writing—review and editing, A.O.; visualization, F.V.; supervision, A.O.; project administration, F.V. and A.O.; funding acquisition, F.V. and A.O. All authors have read and agreed to the published version of the manuscript.

Funding: This research was supported by the German Research Foundation (DFG) via a research grant for the project "Osmotic processes in the cementitious material-reactive resin coating system", grant number 471260929. This is a collaborative project between Bauhaus-Universität Weimar (Weimar, Germany) and the Hamburg University of Technology (Hamburg, Germany).

Data Availability Statement: The original contributions presented in this study are included in the article. Further inquiries can be directed to the corresponding author.

Acknowledgments: Doreen Erfurt (F.A. Finger-Institute for Building Materials Science, Bauhaus-Universität Weimar, 99423 Weimar, Germany) provided support in the preparation and examination of the thin sections and Martin Hampe and Tom Lehmphul (both F.A. Finger-Institute for Building

Materials Science, Bauhaus-Universität Weimar, 99423 Weimar, Germany) provided support in sample preparation and recording of measurements, which is gratefully acknowledged.

Conflicts of Interest: The authors declare no conflicts of interest.

References

1. Klopfer, H. *Anstrichschäden: Strukturen, Verhaltensweisen und Schadensformen von Anstrichen und Kunststoffbeschichtungen*; Bauverlag: Wiesbaden, Germany, 1976; ISBN 3-7625-0738-4.
2. Warlow, W.J.; Pye, P.W. Osmosis as a cause of blistering of in situ resin flooring on wet concrete. *Mag. Concr. Res.* **1978**, *30*, 152–156. [CrossRef]
3. Bode, K.A.; Hofmann, A.; Dimmig-Osburg, A. Zum Einfluss alkalireaktiver Gesteinskörnungen auf die Blasenbildung polymerer Beschichtungen auf Beton. *Bausubstanz* **2011**, *2*, 46–53. [CrossRef]
4. Schulenberg, D. Osmotische Prozesse in Mineralischen Baustoffen. Ph.D. Thesis, Technische Universität Hamburg, Hamburg, Germany, 2024.
5. Wolff, L. Mechanismen der Blasenbildung bei Reaktionsharzbeschichtungen auf Beton. Ph.D. Thesis, Rheinisch-Westfälische Technische Hochschule (RWTH) Aachen, Aachen, Germany, 2009.
6. Schäper, M.; Wächter, B. Vermeidung der Blasenbildung von Reaktionsharzbeschichtungen hinterfeuchteten Betons. In Proceedings of the 18 Internationale Baustofftagung Ibausil, Weimar, Germany, 12–15 September 2012; ISBN 9783000340758.
7. Schäper, M.; Kreye, J.; Hiess, T. *Hinterfeuchtete Betonbeschichtungen—Untersuchungen zur Vermeidung von Osmoseschäden*; Fachhochschule Wiesbaden: Wiesbaden, Germany, 2003.
8. Mühlenbrock, P.; Schubert, H.; Riviere, J. Osmosis Resistant Epoxy Primer. In *Proceedings of the 6 Internationales Kolloquium Industriefußböden*; Technische Akademie Esslingen: Ostfildern, Germany, 2007; pp. 261–268.
9. Schilling, M. Solvent entrapment and osmotic blistering. *JPCL* **2004**, *21*, 24–26.
10. Gaiser, K.J. Empirische Untersuchung über die Korrelation zwischen Restfeuchte und adhäsivem Verhalten von kunstharzgebundenen Primern auf mineralischen Untergründen. In *Proceedings of the Internationales Kolloquium Industriefußböden*; Technische Akademie Esslingen: Ostfildern, Germany, 1991.
11. Schuhmann, H. *Kunstharzbeläge: Mängelfreie Ausführung und Bauphysikalische Grundlagen*; Fraunhofer IRB-Verlag: Stuttgart, Germany, 2005; ISBN 3816765823.
12. Wolff, L.; Raupach, M. Beschichtungsschäden—Schadensmechanismen und Lösungsansätze. In *Proceedings of the 3 Kolloquium Verkehrsbauten, Schwerpunkt Parkhäuser/Brücken*; Technische Akademie Esslingen: Ostfildern, Germany, 2008; pp. 313–324.
13. Ettel, W.-P. *Kunstharze und Kunststoffdispersionen für Mörtel und Betone: Struktur der Polymere; Planung, Bemessung, Prüfung*; Beton-Verlag: Düsseldorf, Germany, 1998.
14. Raddatz, J.; Stenner, R. Blasenbildung unter Reaktionsharzbeschichtungen. In *Proceedings of the Internationales Kolloquium Industriefußböden*; Technische Akademie Esslingen: Ostfildern, Germany, 1999; pp. 545–556.
15. Letsch, R. Blasenbildung bei Kunststoffbeschichtungen auf Beton. In *Proceedings of the Internationales Kolloquium Industriefußböden*; Technische Akademie Esslingen: Ostfildern, Germany, 1999; pp. 527–530.
16. Günter, M. Beanspruchung und Beanspruchbarkeit des Verbundes Zwischen Polymerbeschichtungen und Beton. Ph.D. Thesis, Universität Karlsruhe, Karlsruhe, Germany, 1997.
17. Fiebrich, M. Zur Adhäsion Zwischen Polymeren Bindemitteln und Beton Unter Besonderer Berücksichtigung Von Wassereinwirkungen. Ph.D. Thesis, Rheinisch-Westfälische Technische Hochschule (RWTH) Aachen, Aachen, Germany, 1987.
18. Stenner, R.; Machill, N. Adhäsion und Blasenbildung von Beschichtungen bei rückseitiger Feuchteeinwirkung. In *Proceedings of the Internationales Kolloquium Industriefußböden*; Technische Akademie Esslingen: Ostfildern, Germany, 2003; pp. 79–102.
19. Rheinwald, G. Blasenbildung durch Feuchtigkeit (Osmose). In *Proceedings of the Internationales Kolloquium Industriefußböden*; Technische Akademie Esslingen: Ostfildern, Germany, 1995; pp. 399–406.
20. Rheinwald, G. Osmoseblasen an einer rissüberbrückenden EP-Beschichtung. In *Proceedings of the Internationales Kolloquium Industriefußböden*; Technische Akademie Esslingen: Ostfildern, Germany, 2007; pp. 255–259.
21. Hensel, W. Blasenbildungen bei organischen Beschichtungen auf zementgebundenen Baustoffen. *BFT* **1995**, *61*, 106–114.
22. Yuasa, N.; Sasaki, T.; Matsui, I.; Kasai, Y. Effect of Porosity and Moisture Content of Concrete Slab on Osmotic Blister of Polymer. In *Proceedings of the Internationales Kolloquium Industriefußböden*; Technische Akademie Esslingen: Ostfildern, Germany, 2007; pp. 269–274.
23. Yuasa, N. Surface Layer Concrete. In *Advances in Civil Engineering—Sustainable Materials and Resilient Structures*; Bahadori-Jahromi, A., Ed.; IntechOpen: London, UK, 2024; ISBN 978-1-83769-874-5.
24. Wolff, L. Mechanismen der Blasenbildung bei Reaktionsharzbeschichtungen auf Beton: Ergebnisse eines DFG-Forschungsvorhabens. In *Proceedings of the Internationales Kolloquium Industriefußböden*; Technische Akademie Esslingen: Ostfildern, Germany, 2007; pp. 35–46.

25. Schäper, M.; Kreye, J. Die kritischen Randbedingungen einer Innenbeschichtung Weißer Wannen. *Beton-Stahlbetonbau* **2003**, *98*, 30–41. [CrossRef]
26. Phelps, L. The Case of the Blistering Coating on Tilt-Up Concrete. *CoatingsPro* **2020**, *20*, 90–94. [CrossRef]
27. Engelfried, R.; Eisenkrein-Kreksch, H. *Schäden an Polymeren Beschichtungen*; Fraunhofer IRB-Verlag: Stuttgart, Germany, 2012; ISBN 978-3-81678672-6.
28. Ignoul, S.; van Rickstal, F.; van Gemert, D. Blistering of Epoxy Industrial Floors on concrete substrate: Phenomena and case study. In *ICPIC 04, 11th International Congress on Polymers in Concrete*; BAM: Berlin, Germany, 2004; ISBN 3000137068.
29. Littmann, K. Osmose-Theorie der Bildung von Blasen unter Beschichtungen. *Restor. Build. Monum.* **1999**, *5*, 573–588.
30. Raddatz, J. Osmose unter Beschichtungen. In *Proceedings of the Internationales Kolloquium Industriefußböden*; Technische Akademie Esslingen: Ostfildern, Germany, 2003; pp. 741–744.
31. Nixon, R. Avoiding osmotic blistering in resinous floor coatings. *JPCL* **2004**, *21*, 36–42.
32. Pfaff, F.A.; Gelfant, F.S. Osmotic blistering of epoxy coatings on concrete. *JPCL* **1997**, *14*, 52–65.
33. Reumschüssel, A. Blasenbildungen bei Beschichtungen auf Beton. *VDBinfo* **2010**, *4*, 5–7.
34. Bode, K.A.; Dimmig-Osburg, A.; Moroni, W. Modellversuche zur Blasenbildung polymerer Beschichtungen auf Beton. In Proceedings of the 17 Internationale Baustofftagung, Weimar, Germany, 23–26 September 2009.
35. Schulenberg, D.; Schmidt-Döhl, F.M. Osmotische Prozesse in mineralischen Baustoffen. In Proceedings of the 20 Internationale Baustofftagung, Weimar, Germany, 12–14 September 2018.
36. Schulenberg, D.; Schmidt-Döhl, F.M. Osmotische Prozesse in mineralischen Baustoffen. In Proceedings of the Tagung Bauchemie der GDCh Fachgruppe Bauchemie, Aachen, Germany, 30 September–2 October 2019.
37. Diederichs, U.; Jäntsch, S.; Sklenářová, D. Causes of Blistering in Plastic Coatings on Screeds and Concrete. *AST* **2021**, *109*, 53–58.
38. Gray, M. Defining Osmotic Blisters and Causes in Resinous Floor Coatings. In Proceedings of the SSPC 2015 Greencoat, Las Vegas, NV, USA, 3–6 February 2015; pp. 1–9.
39. Aher, S.; Devillers, P.; Fau, G.; Buisson, C. Blistering of Industrial Floor on Concrete Substrate: The Role of the Air Overpressure. In Proceedings of the COMSOL Conference, Paris, France, 17–19 November 2010.
40. Wolff, L.; Raupach, M.; Hailu, K. Ursachen der Blasenbildung bei Reaktionsharzbeschichtungen auf Beton—Welche Rolle spielt die Osmose? *Beton-Stahlbetonbau* **2007**, *102*, 439–449. [CrossRef]
41. Maj, M.; Banera, J. Durability of protective coatings of reinforced concrete surfaces in tanks for chemically aggressive liquids. *Mater. Bud.* **2025**, *637*, 61–68. [CrossRef]
42. Banera, J.; Maj, M. Reasons for lack of adhesion of polyurea coatings to concrete substrates in chemically aggressive water tanks. *Mater. Bud.* **2024**, *628*, 20–26. [CrossRef]
43. German Committee for Structural Concrete (DAfStb). *Schutz und Instandsetzung von Betonbauteilen: Teil 2: Bauprodukte und Anwendung*; Beuth Verlag GmbH: Berlin, Germany, 2001.
44. Günter, M. Polymerbeschichtungen auf Beton—Betonspezifische Beanspruchung und Beanspruchbarkeit des Verbundes. In Proceedings of the 24 Forschungskolloquium des Deutschen Ausschusses für Stahlbeton, Karlsruhe, Germany, 11–12 October 1990; pp. 111–116.
45. Rheinwald, G. Blasenbildung an Beschichtungen durch Substratreaktion. In *Proceedings of the Internationales Kolloquium Industriefußböden*; Technische Akademie Esslingen: Ostfildern, Germany, 2003; pp. 733–740.
46. Molkenthin, A.; Wilsch, G.; Huckebrink, D. Frühreaktionen beim Beschichten von Betonflächen mit Neigung zur Alkali-Kieselsäure-Reaktion. In *Proceedings of the Kolloquium Verkehrsbauten, Schwerpunkt Parkhäuser*; Technische Akademie Esslingen: Ostfildern, Germany, 2010.
47. Wolff, L.; Harnisch, J.; Raupach, M. Beurteilung komplexer Schadensbilder bei Meerwasserbauten am Beispiel einer Anlegerbrücke. In *Proceedings of the Kolloquium Erhaltung von Bauwerken, 27–28 January 2009*; Technische Akademie Esslingen: Ostfildern, Germany, 2009; pp. 295–301.
48. Helmuth, R.; Stark, D.; Diamond, S.; Moranville-Regourd, M. Alkali-Silica Reactivity: An Overview of Research, Washington, DC, USA. 1993. Available online: https://onlinepubs.trb.org/onlinepubs/shrp/SHRP-C-342.pdf?utm_source=chatgpt.com (accessed on 26 February 2025).
49. Giebson, C. Die Alkali-Kieselsäure-Reaktion in Beton für Fahrbahndecken und Flugbetriebsflächen unter Einwirkung Alkalihaltiger Enteisungsmittel. Ph.D. Thesis, Bauhaus-Universität Weimar, Weimar, Germany, 2013.
50. Hofmann, A. Einfluss von Gesteinskörnungen auf die Blasenbildung von Beschichtungen auf Beton. Diploma Thesis, Bauhaus-Universität Weimar, Weimar, Germany, 2010.
51. Bogue, R.H. Calculation of the Compounds in Portland Cement. *Ind. Eng. Chem. Anal. Ed.* **1929**, *1*, 192–197. [CrossRef]
52. *DIN EN 196-1*; Methods of Testing Cement–Part 1: Determination of Strength. DIN German Institute for Standardization: Berlin, Germany, 2016.
53. *DIN EN 1015-3*; Methods of Test for Mortar for Masonry—Part 3: Determination of Consistence of Fresh Mortar (by Flow Table). DIN German Institute for Standardization: Berlin, Germany, 2007.

54. *DIN EN 1015-7*; Methods of Test for Mortar for Masonry—Part 7: Determination of Air Content of Fresh Mortar. DIN German Institute for Standardization: Berlin, Germany, 1998.
55. *DIN EN 1015-11*; Methods of Test for Mortar for Masonry—Part 11: Determination of Flexural and Compressive Strength of Hardened Mortar. DIN German Institute for Standardization: Berlin, Germany, 2020.
56. Stark, J.; Wicht, B. *Zement und Kalk: Der Baustoff als Werkstoff*; Birkhäuser: Basel, Switzerland; Boston, MA, USA; Berlin, Germany, 2000; ISBN 9783764362164.
57. *DIN EN ISO 527-1*; Plastics—Determination of Tensile Properties—Part 1: General Principles. DIN German Institute for Standardization: Berlin, Germany, 2019.
58. *DIN EN ISO 62*; Plastics—Determination of Water Absorption. DIN German Institute for Standardization: Berlin, Germany, 2008.
59. *DIN EN ISO 7783*; Paints and Varnishes—Determination of Water-Vapour Transmission Properties—Cup Method. DIN German Institute for Standardization: Berlin, Germany, 2019.
60. ImageJ. Available online: https://imagej.net/ij/ (accessed on 5 February 2026).
61. Ehrenstein, G.W.; Riedel, G.; Trawiel, P. *Praxis der Thermischen Analyse von Kunststoffen*; Hanser: München, Germany, 2003; ISBN 3-446-22340-1.
62. Hardis, R.; Jessop, J.L.; Peters, F.E.; Kessler, M.R. Cure kinetics characterization and monitoring of an epoxy resin using DSC, Raman spectroscopy, and DEA. *Compos. Part A Appl. Sci. Manuf.* **2013**, *49*, 100–108. [CrossRef]
63. Nielsen, L.E. Cross-linking–effect on physical properties of polymers. *J. Macromol. Sci. Part C* **1969**, *3*, 69–103. [CrossRef]
64. Zhao, C.; Wen, R.; Dai, Y.; Al-Mansour, A.; Fu, C.; Zeng, Q. Hydrolysis degradation mechanisms of epoxy resin coatings on concrete in hydrothermal environment resolved by molecular dynamic simulations. *Const. Build. Mater.* **2025**, *479*, 141463. [CrossRef]
65. Xian, G.; Niu, Y.; Qi, X.; Tian, J.; Li, C.; Yue, Q.; Guo, R. Water absorption and property evolution of epoxy resin under hygrothermal environment. *J. Mater. Res. Technol.* **2024**, *31*, 3982–3997. [CrossRef]
66. González-Benito, J.; Bravo, J.; Mikes, F.; Baselga, J. Fluorescence labels to monitor water absorption in epoxy resins. *Polymer* **2003**, *44*, 653–659. [CrossRef]
67. Guo, R.; Li, C.; Xian, G. Water absorption and long-term thermal and mechanical properties of carbon/glass hybrid rod for bridge cable. *Eng. Struct.* **2023**, *274*, 115176. [CrossRef]
68. Chin, J.W.; Nguyen, T.; Aouadi, K. Sorption and diffusion of water, salt water, and concrete pore solution in composite matrices. *J. Appl. Polym. Sci.* **1999**, *71*, 483–492. [CrossRef]
69. *DIN EN 1504-2*; Products and Systems for the Protection and Repair of Concrete Structures—Part 2: Surface Protection Systems for Concrete. DIN German Institute for Standardization: Berlin, Germany, 2005.
70. Romberg, H. Zementsteinporen und Betoneigenschaften. *Beton-Informationen* **1978**, *5*, 50–55.
71. Beddoe, R.; Springenschmid, R. Feuchtetransport durch Bauteile aus Beton. *Beton-Stahlbetonbau* **1999**, *94*, 158–166. [CrossRef]